A Cellular Automaton – Based System for the Identification of Topological Features of Carotid Artery Plaques

Submitted for the Degree of Doctor of Philosophy
At the University of Northampton

2014

Matthew Allan Burley Delaney

Contents

Page Number

Figures

Page Number

Chapter One

Chapter Two

Chapter Three

Chapter Four

Chapter Five

Tables

Page Number

Chapter Two

Chapter Three

Chapter Five

List of abbreviations

APL A Programming Language
AI Artificial Intelligence
ARFI Acoustic Radiation Force Imaging
ART Algebraic Reconstruction Technique
CA Cellular Automaton
CDN Condition
CH Choose
CL Classical Logic
CP Cannot Proceed
DCA Driven Cellular Automaton
EIT Electrical Impedence Tomography
EPI Extreme Physical Information
GA Genetic Algorithm
GaL Geometric Algebra
GEL Geo-entropic Logic
GP General Practitioner
MRI Magnetic Resonance Imaging
PC Personal Computer
PDF Probability Density Function
RSE Ring Sum Expansion
SNR Signal to Noise Ratio
TIA Transient Ischaemic Attack
VAF Virtual Abstract Function

Acknowledgements

I would like to thank Professor Kamal Bechkoum and Dr Gillian Pearce for their advice and support throughout this project along with Professor Phil Picton who helped get me settled into a completely new institution in record time. Additional thanks must go to Mr David Luckhurst for producing much more attractive 3D renderings of my data than I ever could and to my wife Colleen Delaney for her moral support, laboratory assistance and proofreading of this thesis.

Abstract

The formation of a plaque in one or both of the internal carotid arteries poses a serious threat to the lives of those in whom it occurs. This thesis describes a technique designed to detect level of occlusion and provide topological information about such plaques. In order to negate the cost of specialised hardware, only the sound produced by blood-flow around the occlusion is used; this raises problems that prevent the application of existing medical imaging techniques, however, these can be overcome by the application of a nonlinear technique that takes full advantage of the discrete nature of digital computers. Results indicate that both level of occlusion and presence or absence of various topological features can be determined in this way.

Beginning with a review of existing work in medical-imaging and in more general but related techniques, the EPI process of Friden (2004) is identified as the strongest approach to a situation where it is desirable to work with both signal and noise yet avoid the computational cost and other pitfalls of established techniques. The remained of the thesis discusses attempts to automate the EPI process which, in the form given by Frieden (2004), requires a degree of human mathematical creative problem-solving. Initially, a numerical-methods inspired approach based on genetic algorithms was attempted but found to be both computationally costly and insufficiently true to the nature of the EPI equations. A second approach, based on

the idea of creating a formal system allowing entropy, direction and logic to be manipulated together proved to lack certain key properties and require an amount of work beyond the scope of the project described in this thesis in order to be extended into a form that was usable for the EPI process.

The approach upon which the imaging system described is ultimately built is based on an abstracted form of constraint-logic programming resulting in a cellular-automaton based model which is shown to produce distinct images for different sizes and topologies of plaque in a reliable and human-interpretable way.

Chapter One

Introduction

1.0 Introduction

The formation of a plaque in one or both of the internal carotid arteries poses a serious threat to the lives of those in whom it occurs. The usual result of such a condition is the restriction of blood-flow to the brain, a condition which is particularly devastating should a piece of the plaque be broken off as its arrival in the brain may lead to a stroke. Commonly however, ischaemic attacks otherwise known as TIAs or mini-strokes may occur. In such an event the GP may refer the patient to hospital for examination by ultrasound (USS) which, by means of Doppler-reconstruction can approximate the level of occlusion present in the artery. While this information is useful from a diagnostic point of view, the surgery which normally results from a positive identification of carotid atherosclerosis is not without risk since the topological and geometric nature of the plaque is unknown until the incision is made. A worst case scenario of this relative lack of information would be the detachment of a piece of the plaque which would then travel up into the brain potentially causing the patient to stroke whilst on the operating table. Carotid atherosclerosis is not an uncommon condition; in seven US states during the period 1989 to 1996 almost 300,000 carotid endarterectomies were performed (Gross *et al.*, 2000).

The primary motivation for this project, as described above, is longitudinal in

nature, seeking to improve an existing medical procedure, however during the construction of the project's proposal, it became clear that a lateral motivation was also possible – that of reducing the cost of the equipment involved for plaque detection and imaging to the point at which it would be possible to perform diagnoses in the GP's surgery; this would provide the benefit of early detection, increasing the patient's chance of survival both in terms of the condition and in any resultant surgical procedure.

The purpose of this thesis is to describe the methodology that has been developed in order to solve the problem of carotid atherosclerotic plaque imaging from one-dimensional acoustic data. Chapter two outlines the primary research question and highlights those problems specific to solving it. This is followed by a literature review covering all relevant areas of computer science, mathematics and physics in order to put the proposed approach in context and justify a decision, made early on in the project's time-scale, not to take the usual deterministic approach of most medical imaging systems. Chapter four describes the general methodology used to investigate multiple candidate approaches to solving the problem and the results of these subsequent investigations are covered in the following chapters. The results of the final, successful approach are described and analysed in chapters eight and nine with chapter 10 summarising the conclusions drawn.

1.1 Aims of the study

This study forms the second phase of development of a system designed to help prevent strokes by the early detection and analysis of atherosclerosis (the formation of plaques in the carotid arteries which supply blood to the brain). Such blockages can develop as a result of a fatty diet, the lipids (fatty deposits such as cholesterol) building up over time (Robbins *et al*, 2005). The chances of this occurring are increased by smoking (a habit shared by approximately 1.3 billion people worldwide (World Health Organisation, 2004)) as the carcinogens present in tobacco damage the artery lining thus creating a site at which a plaque can form. Although surgery, in the form of a Carotid Endarterectomy operation, provides a solution in many cases, this option is high-risk and is usually only taken once clinical symptoms present and the plaque, which is causing 75% or more occlusion by this time, has been detected and analysed by an ultrasound scan. One way to provide earlier detection of the condition would be to provide ultrasound scanning equipment in GPs surgeries but the increased cost of the equipment for a condition that is not among the most common that the average GP will see, combined with the difficulty in extracting useful images of plaques using ultrasound means that this approach remains unlikely to be take up by the majority of doctors. In any case, portable ultrasound machines are usually used for abdominal scans and still require an operator who has had training in this kind of diagnosis. The cost of such an option would be around £3,000 not including the wages of the operator. Standard ultrasound

machines start at £10,000 and go up to as much as £125,000. Even if a machine at the lower end of this price range were to be usable for carotid artery plaque detection, it would still be cost prohibitive for most GPs.

During the first phase, a system was developed that, rather than using ultrasound, scans passively by analysing the sound caused by blood flowing through the carotid artery. Turbulence caused by the presence of a plaque shows up on a Fourier spectrograph (which shows the component frequencies or 'partials' of a waveform) and by producing a general model of the relationship between Fourier spectrograph and level of occlusion, it is possible to provide an automated indication of the latter for any new example presented to the system.

An additional benefit of this technique is that the task of ascertaining the position of a plaque becomes more automated compared to ultrasound systems which rely entirely upon the operator for this.

Figure 1.1: Sound being produced by turbulence in an occluded carotid artery

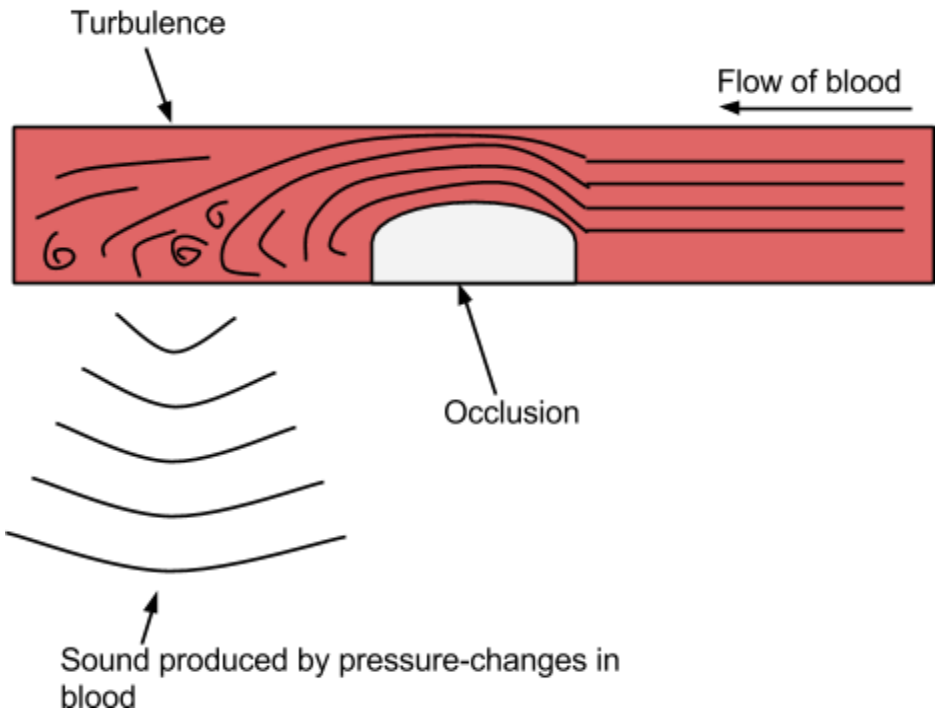

While prior knowledge of the size and location of the plaque is extremely useful to surgeons, it would be even more advantageous to have an idea of the topological features of a particular blockage and the two main questions for this project are therefore 1) How such features can be categorised and detected, providing the surgeon with a 'property-sheet' relating to a particular plaque and 2) How a three-dimensional image of the plaque can be generated in order to further assist the surgeon in planning carotid endarterectomies. The fundamental issue that must be overcome in order to answer either of these questions is that of the dimensionality of the data with which the system works.

1.2 Research question

Considering that the cost of processing naturally occurring sound is the same as that of a modern PC, is the production of three-dimensional models of carotid artery plaques based only on the sound of turbulence caused by blood passing over and around such occlusions feasible and, if so, to what extent? Since the sound in question is produced entirely by the phenomenon and needs only to be recorded and processed, the additional cost and complexity in, for instance, ultrasound systems would be nullified if this question can be answered to a sufficiently positive extent.

1.3 Aims and objectives

Aim: Develop a deep understanding of existing medical imaging techniques in order to ascertain which, if any, may be applicable to the problem dealt with in this study and to identify gaps in knowledge.

Objective: Review existing medical imaging technologies and techniques (regardless of area of physiological application) to determine what, if anything, might be of use in answering the research question.

Objective: Review work from areas that are not specifically related to

medical imaging but may be of use in the case of this project.

Aim: Construct a developmental and experimental methodology for the creation and practical application of a medical imaging approach to carotid artery plaque analysis.

Objective: Design a method of producing data on which to test a prototype system which is on-demand and can be steered toward different variations of the problem.

Objective: Investigate a broad spectrum of approaches and determine which is likely to be the most successful.

Aim: Produce a prototype system based upon the chosen approach and critically examine its output with regard to providing information about plaque topology.

Chapter Two

Literature survey and limitations of current techniques

2.0 Literature survey and limitations of current techniques

Central to the nature of the project (that of producing a low-cost imaging device using standard PC hardware) is the way in which acoustic data will be collected from outside of the carotid artery. A microphone will record the sound of turbulence in the bloodstream and thus the data received by the imaging algorithm will be a one-dimensional sequence of amplitude values. This makes the process of topological feature identification more difficult than in other medical imaging systems as there is no way to 'triangulate' in on a particular point via multiple sensors. As the significance of this is more apparent if one has an understanding of existing medical-imaging technology, a survey of relevant literature will now be given.

2.1 Medical imaging

2.1.1 Magnetic Resonance Imaging

Turning first to the field of medical imaging as it is currently established, we find that existing systems tend to have one or both of two important factors: 1) A measure of control over or a directed external source of energy and 2) Multiple sensors. As a first example, consider Magnetic Resonance Imaging (MRI). This works by aligning the body's protons in a magnetic field, then relaxing this field in

order to generate waves of released energy (Schempp, 1998) (see also Damadian (1971) and Mansfield (1977)) which are then broken down into their Fourier Spectrograms. The spectrographic information can then be used to create an image of the area which was scanned.

MRI has been applied to the problem of 3D imaging of carotid-artery plaques by Sakellarios *et al.* (2012) but the cost of the equipment necessary rules out the use of MRI in general for this project.

2.1.2 Computed Tomography

Another established imaging system is X-Ray Computed Tomography. This utilises a cone-shaped beam of X-rays which are projected through the body to sensors which measure their intensity at different locations. From these intensity measurements one usually applies the Radon transform (Radon, 1917) in order to work out the density of the attenuating material at specific coordinates in the chosen 2D slice that contributed to the overall intensity reading. As with the Fourier transform, computational complexity has resulted in research designed to improve the efficiency of the Radon transform (see for example Brady (1998)) and has perhaps been a driving force in the development of the Algebraic Reconstruction Technique (ART) (Raparia *et al.*, 1997) which effectively amounts to the same concept and, in fact, serves as a gentler introduction to the principle than Radon's

original paper.

So far then, two systems have been summarised. Both use external sources of energy that they have a measure of control over. A third example demonstrates that if this aspect is reduced, the computational complexity may go down whilst hardware complexity goes up.

2.1.3 Electrical Impedance Tomography

Electrical Impedance Tomography (EIT) (Barber and Brown, 1984) works by applying electrical currents to the tissue being studied and measuring the corresponding voltages which will have been affected by the resistivity of the tissue, that resistivity being used to diagnose certain conditions. To quote Vauhkonen *et al.* (1996): "EIT image reconstruction is a nonlinear ill-posed inverse problem for which reason we have to use regularization techniques to obtain stable solutions."

The most popular approach to this regularization seems to be that of Tikhonov (1963) in which a regularization matrix and parameter are used to provide a numerical kernel against which the potential differences based upon tissue density are minimised. From the point of view of this project, it is very reassuring that, given the complexity of the problem which is close to that to be dealt with in this project, a relatively simple mathematical technique can make the data usable for diagnosis.

2.1.4 Ultrasound

The current standard way of identifying Carotid Atherosclerosis in patients who have presented to their GP with appropriate symptoms is by Doppler Ultrasound. This is effectively a second-order measurement in that occlusion is identified by the variance in velocity of the blood flowing through the artery achieved by detecting Doppler Shift by a method which will now be summarised from the form in which it is given in (Hedrick *et al.*, 1995). An ultrasound transmitter and receiver are paired in a surface probe which is placed on the side of the neck. The frequency of the soundwaves returning from inside the artery is altered by the Doppler effect inferred by the movement of the blood. The altered wave is combined with the original soundwave, the differing frequencies introducing 'beats' or pulses of significant amplitude. The metrics of the beats can then be used to calculate the speed at which the blood is flowing. An occlusion in the carotid artery causes several stages of distortion to the otherwise transverse flow of the blood; these cause variations in the velocity of said blood and the position and size of the occlusion can thus be computed.

Work specifically targeting the problem of imaging carotid-artery plaques using ultrasound has been undertaken by various authors but the requirement of a

directed energy source and the specialised hardware needed in order to produce it makes their techniques inapplicable to the context of this project. It is, however, worth noting that Dahl *et al.* (2009) obtained high-resolution two-dimensional images of both homogeneous and heterogeneous plaques but their approach uses Acoustic Radiation Force Impulse (ARFI) imaging which requires directed energy, i.e. special hardware. The images produced by their system also require interpretation by an expert in order to provide clear information about plaque topology. Fenster *et al.* focus on characterizing plaque morphology but, again, used directed energy in order to do so.

The principles of Doppler Ultrasound and, in fact, Ultrasound in general are of no major use to this project as they require specialist hardware (transmitter and receiver) and in any case are not ideally suited to the degrees of freedom required of a 3D model of something as small as an arterial plaque in such a way that a surgeon can rotate and translate the model on the screen. This project's approach is to work with what information is inferred by the smallest number of variables possible; currently just one variable: acoustic pressure. In Doppler-based systems, the sound from inside the artery is reproduced from the beats and could therefore be used as input to the system but this would invalidate the project's requirements of affordability and minimal dependency on specialist hardware.

2.2 Acoustic detection

As has been discussed in the preceding sections, the applicability of existing medical imaging techniques to the problem of atherosclerotic plaque imaging based upon one-dimensional data is minimal. Because of this, a broad survey of acoustic data analysis has been carried out in order to provide a picture of the general approaches being taken. As before, these approaches often involve controlled or generated energy, multiple sensors, or both but the mathematical and computational techniques used are sometimes of interest.

An obvious avenue to explore is that of Fourier Spectrogram analysis but it is felt that the fundamental research question of this project (that of producing an image based upon turbulent vortex sound) would be better addressed by an emphasis on discrete computation rather than mathematical analysis which is continuous in nature. This is borne out by work such as that of Dellandrea *et al.* (2002) where the detection of gastro-oesophageal reflux is approached not by analysing raw data from Fourier analysis, but from the reduction of the raw data into a metric based on Zipf's law (Zipf, 1949) which is rationalised for the phenomena being measured. Zipf's law is in many respects a comforting reassertion of the old idea that there is innate order in the Universe. As it is applied in Dellandrea *et al's* work, it is related to the Golden Section of the Ancient Greeks, providing an anchor point in the n-space of acoustic metrics, their combinations and permutations against which to compare our physical

examples. An approach such as this may be useful if it provides a way of identifying general topological features of atherosclerotic plaques. Such an approach would have a possible advantage over techniques such as Principle Component Analysis (discussed below) in that computing log-log graphs in order to perform a 'Zipfian'-analysis is far less computationally expensive than such techniques.

In other work on acoustic data analysis, we find that more use of stochastic and Artificial Intelligence (AI) techniques is made. This places the responsibility of finding an appropriate representation of the data to the computer and, as a side effect of the approximate nature of such techniques, also takes away the need to deal explicitly with noise and other metric errors present in the recorded sound. An excellent demonstration of such a fusion of techniques is provided by Wang & Qi (2002) who supplement Spectrogram and Wavelet -based techniques with Principle Component Analysis, Minimum Distance and k-Nearest Neighbour algorithms in order to classify military targets from distributed acoustic sensors. These techniques are all, basically, designed to organise data into meaningful categories without the intervention of the user although in the case of Principle Component Analysis it is perhaps more correct to say that the data stays as it is and the axes on which it is plotted are altered so that they represent the dominant 'features'.

The more traditional approach of Venkatesen *et al.* (1997) combines Fourier analysis with classification based upon eigenvectors and is purported to be

sufficiently accurate to allow automatic monitoring of faults in helicopter rotors – a problem hampered by considerable ambient noise. The eigenvector approach is not dissimilar to Principle Component Analysis in that eigenvectors tell us the direction in which the matrices from which they are derived 'lean', i.e. what their most 'natural' direction is. All of this lends weight to the argument that will form a large part of the basis for this project: That if there is order in a data-set then stochastic and AI techniques combined with attention to the level of entropy in the data as these techniques are applied is highly likely to find it.

2.3 Numerical methods

2.3.1 Review of use in medical imaging

Having decided upon a combination of traditional mathematical and more approximating techniques, the next logical step was to survey the use of such techniques in the practical implementation of various medical imaging techniques. Fortunately an excellent survey of this area is provided by Natterer (1999) who covers the techniques currently in use in the fields of X-ray Tomography (discussed above), Nuclear Medicine (based upon the detection of, for instance, photons generated by the injection of a radioactive isotope into the bloodstream), MRI and electron microscopy. What Natterer does not cover is the area of Ultrasound imaging which would, on the surface, appear far more relevant to the subject of this project.

However, image reconstruction in ultrasound systems is based upon the Doppler effect, making the hardware and reconstructive algorithms very different from what we require. The integral-transform based approach taken by the systems reviewed so far are therefore more relevant.

2.3.2 Kalman Filters

For problems where something is known about the physical process being modeled and where one is working with noisy data, the Kalman Filter (Kalman, 1960) is a well established technique. The known mathematical relationship(s) of the phenomenon are combined with actual measurements to produce a best guess of the underlying system at a particular point in time. While the original version of the filter suffers from high computational cost (Lopes and Piedade, 2000) for multivariate problems and is known to have problems modelling nonlinear phenomena (Julier and Uhlmann, 1997), variations of the technique such as the Ensemble Kalman Filter (Evensen, 1994) have been developed to overcome these limitations.

For the problem being dealt with by this project, a Kalman Filter-based technique would involve the relevant equations for vortex-sound being used as an ideal model. The filter would then be supplied with measurements of the sound recorded from a physical plaque simulation, with the mathematical model recalculated at each time-interval to keep the two sources of data synchronized. The Kalman Filter is designed to take these two sources of data about a phenomenon and

produce an estimate of the system's state that is better than either on its own.

2.3.3 Other relevant

At the root of the field of numerical methods is a technique known as Lagrange Interpolation. This has been expanded using Geometric Algebra (see 3.5 below) to create a multivariate interpolation algorithm that allows us to produce approximating equations that are more easily invertible than their vector-algebra equivalents.

Whilst the 'core' physics of sound generated by the motion of a fluid were introduced by Lighthill (1952) and surveyed by Howe (2003), the relationship between fluid turbulence and acoustic pressure variation is given in a directly computable form as a vector-algebra equation by Dobashi *et al.* (2004). This formula (and the algorithm which makes use of it) is intended to simulate vortex-sound in computer games based upon the turbulence at a specific point (called a *voxel*) in the flow. We require the opposite but face two obstacles: 1) The equations described by Dobashi *et al.*(2004) are formulated using vector-algebra operators which are not invertible due to the nature of the vector dot-product and 2) They are only an approximation to vortex-sound in any case since the measure of success is their ability to produce sound that gamers find realistic; using them for this project, even in inverted form could therefore potentially lead us astray.

2.3.4 Extreme Physical Information

The principle of Extreme Physical Information (also known as the Frieden-Soffer principle) is effectively a method of deriving Lagrangians using elements of information theory and the calculus of variations. Described fully with example applications in the book "Science from Fisher Information" (Frieden, 2004), it hinges upon the concept of measurement resulting in a loss of information. The measure of information used is that proposed by geneticist Ronald Fisher and, while similar in form to Shannon's form of entropy (Brillouin, 2004) (which itself can in some cases be the Boltzmann Entropy of thermodynamics (Frieden, 2004)), it has the property of being locally dependent upon the phenomenon being measured. This means that the order of data-points in a data-set affects the amount of Fisher Information that that data-set has but not the amount of Shannon Entropy (compare equations 2.1 and 2.2 below).

$$I = \int dx.p'^{2}(x)/p(x) \qquad \textbf{(2.1)}$$

$$H \equiv \int dx.p(x) ln\ p(x) \qquad \textbf{(2.2)}$$

Frieden postulated that by using the calculus of variations to minimise the information lost during measurement, it could be possible to derive the Probability Density Function (PDF) of the phenomenon in question. His book (cited above)

contains numerous applications of this technique; these include both EPI derivations of existing physical laws as well as new ones.

The EPI principle has been criticised (Lavis and Streater, 2002) on, the grounds that the applications cited by Frieden require a degree of mathematical creativity that suggests that the principle only works if one has more advance knowledge of the phenomenon being measured than would normally be the case. On the other hand, this could also be said of Classical Measurement Theory (the theory that EPI is intended to replace) it often being the case that "It usually happens that the differential equations for a given phenomenon are known first, and only later I the Lagrange function found, from which the differential equations can be obtained." (Morse and Feshbach, 1953).

While Frieden's book serves as the only introduction to the subject, the examples of it's application are almost all in the area of Physics and therefore somewhat inaccessible to those who want to cement their understanding of the principle. There are, however, two applications that have been made since the book's publication that provide more accessible applications to the concept. The first of these is that of Menard and Eboueya (2002) who use the EPI equation I – J = extremum as an objective function in the problem of fuzzy clustering (in which the data-points given to the system are organised into groups based on a user-defined measure of their similarity). This work is actually very close to that proposed by this

project with the exception that a formula for the bound information J is available in the clustering application whereas in this project it is not. Nevertheless, Menard and Eboueya's work takes the continuous mathematics of Frieden's book and provides discrete equivalents to the concepts involved or at least more easily discretisable continuous versions.

A second application is that of Frieden and Gatenby (2005) in which the EPI principle is used to derive allometric laws of the form $y = Yx_a$. These laws are obeyed by many living and non-living systems for a small range of values for a. This paper is considerably clearer on the distinction between information measures I and J than that of Menard and Eboueya and the mathematics involved is less specific to the science of Physics than that required in order to understand earlier applications.

2.4 Genetic algorithms

A Genetic Algorithm (GA) is an artificial intelligence technique which attempts to solve problems by simulating biological evolution to some degree. A basic genetic algorithm will have a pool of chromosomes which represent solutions to the problem, a fitness function which is used to evaluate those chromosomes and the ability to cause mutation and crossover (where two chromosomes exchange a sub-set of their genes). There is a myriad of variations on this basic design and it is often the case that specific variation will be designed to improve the efficiency of a

genetic algorithm in solving a particular problem or class of problems, the biggest obstacle often being premature convergence (convergence on a local-maximum of the search-space). A thorough introduction to GAs is given by Mitchell (1996) who covers the most commonly used techniques of solution-encoding, selection methods and genetic operators as well as their parameters such as mutation and crossover rates. It may well be the case that a particular GA implementation can be 'fine-tuned' by adjusting any one aspect of the basic algorithm or a combination of several. For this reason, it is felt that a detailed investigation of more unusual GA components should be driven by knowledge of the specific needs of the system being developed.

2.5 Geometric algebra

It is widely known that working with vectors, or simply multivariate data-sets often requires at some level that the individual coordinates (or data-values) are treated as individual entities. This can result in an increase in the complexity of data-processing systems, especially at design-time resulting in longer development times an increased risk of bugs. In the latter half of the twentieth century, an alternative to vector-algebra began to gain in popularity; Geometric Algebra (or GaL) is Hestenes and Sobczyk's (1984) interpretation of an anti-commutative algebra developed by the noted mathematicians William Kingdom Clifford and Hermann Grassman. Whilst Geometric Algebra is of interest in a number of areas of pure mathematics, from the point of view of this project, potential benefits resulting

from the unification of scalars, vectors, complex numbers and quaternions were apparent.

We will restrict ourselves to that instance of the algebra best pertaining to physical space: $G_{3,1}$, that is to say a geometric algebra with a three-dimensional basis over the real numbers. The first thing to note is that this results in *eight* linear dimensions:

Figure 2.1: Illustration of linear dimensions.

1

e1 e2 e3

e1 ^ e2 e2 ^ e3 e1 ^ e3

e1 ^ e2 ^ e3

so that a variable x in $G_{3,1}$ has eight 'coordinates', each of which can be set independent of the others. The relationships between the linear dimensions are provided by the algebra's operators. Addition and subtraction work in exactly the same way as they do in vector-algebra, multiplication does not. Geometric Algebra defines the Geometric Product as uv = u · v + u ^ v. That is, for *pseudoscalars* (the term given to values from a geometric algebra) u and v, the geometric product is the sum of their dot-product and their wedge-product. The dot-product is the same as that defined in vector-algebra. The wedge product is similar to the cross-product of

vector-algebra except that the result is not a vector, but an oriented area known as a multivector (see Fig. 2.2).

Figure 2.2: Illustration of and equation for magnitude of wedge-product.

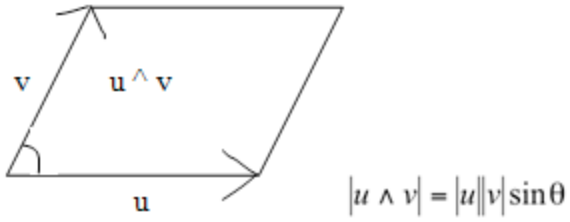

Therefore, the wedge product of vectors u and v having geometric coordinates (1,2,3) and (1,3,5) is (1 * e_1^e_2, 2 * e_2^e_3, 1 * e_1 ^ e_3).

As was stated above, GaL is an anticommutative algebra; this means that for two pseudoscalars a and b, ab = -ba. It is this property that provides the two important crossovers that make GaL applicable to a wide range of physical problems: Firstly, the anticommutative product models the behaviour of vectors and secondly, the area of the wedge product will always be an imaginary number because $(e_i e_j)_2$ = -1; this property means that the geometric product effectively produces a hyper-complex number and we can therefore treat scalars, complex numbers, quaternions and octonians as identical objects (at least for the purposes of algebraic manipulation). A good illustration of how this works is provided by the expressions for the dot and cross-product operators of vector-algebra:

$$a \cdot b = (ab + ba) * 0.5 \qquad \textbf{(2.1)}$$

$$a \times b = (ab - ba) * 0.5 \qquad \textbf{(2.2)}$$

Naturally, the individual Euclidean coordinates of a and b must be dealt with individually at some level for actual numerical evaluation but this can be dealt with by computer-software.

2.5.1 A review of Geometric Algebra implementations

There are currently two reasonably mature implementations of geometric algebra available: The first allows the programmer to treat pseudoscalars as primitive data-types whereas the second takes a pure, monadic object-oriented approach.

2.5.1.1 C++

One of the most flexible implementations of geometric algebra is the nklein library (nklein software, 2000). Written in the C++ programming language, the library was able to utilise template metaprogramming at a time when it was not supported in Java (the language of the other implementation). This approach to

implementing GaL in a programming language allows GaL 'objects' to be treated in the same way as one would treat integers or floating-point numbers.

Figure 2.3: Example nklein code.

```
// Store the wedge-product of pseudoscalars x and y in a new
// variable z
nklein::GeometricAlgebra<double, 3> z = x ^ y;
```

A denary indexing scheme is used to provide access to the underlying coordinates such that z[0] is the scalar part of the pseudoscalar, z[1], z[2] and z[4] store the x, y and z coordinates and the remaining linear coordinates are stored at indices which are combinations of these (i.e. the value for $e_1 \wedge e_2$ is stored in z[3]).

This library is the most flexible and highly integrated discovered by the author to date but would be rather difficult to map to most other languages due to it's reliance on both template classes and operator overloading.

2.5.1.2 Java

In addition to not using template metaprogramming, Java does not support operator-overloading and subsequently the Java implementation of GaL cannot provide the same seamlessness as the nklein library. Nevertheless, a full-featured implementation is available in the form of Clados (Differ, 2002). This implementation seems to be aimed at the area of computer-graphics being restricted to three-linear dimensions but, within this space, still provides most of the benefits of GaL with the added advantage of being platform independent. The equivalent of the code given above is shown in Fig. 2.4.

Figure 2.4: Example Clados code

```
// x becomes the wedge-product of itself and y
x.Wedge(y);
```

The indexing scheme used by Clados will be more comfortable to Fortran programmers than that of nklein, the linear dimensions simply being index by the numbers 1 to 8.

2.6 Dimensional and configurational-analysis

A common approach to problem-solving and solution-verification in engineering and physics is the use of *dimensional-analysis*. In short, the technique involves working not with variables as indicators of quantity but with the dimensions of those quantities. A simple example would be the situation in which, given the velocity of an object in meters per second and a travelling time in seconds, we want to calculate how far the object will have travelled in that time. We decide to multiply the velocity by the travelling time but how do we know that that is the correct operation? Formal proof via algebra would of course be one way but another is to verify that the result of the calculation will be a quantity in meters:

$$\left(\frac{m}{s}\right) s = m \qquad \textbf{(2.3)}$$

This example is of course too simple to warrant such attention in reality but the technique of dimensional-analysis has been used to quickly provide insight and verify solutions for very complex physical phenomena and, as a result, has become a field of study in itself with an extension of the theory being used to calculate the expansion of the explosions created by the first atomic bombs (Barenblatt, 1996).

In terms of increasing the level of abstraction involved in dimensional-analysis whilst still retaining usefulness and mathematical rigour, the

work of Becker (1976) defines the concepts of *eigenratio* and *configuration*. An eigenratio is, simply a pair of quantities which can be identified as coupled in some way such that their pairing is informative when examining a physical phenomenon. A configuration is a set of eigenratios and, with these highly abstract concepts, Becker shows that it is possible to reason in useful, in-depth ways about various physical phenomena. This technique is known as *configurational-analysis.*

2.7 Cellular automata

The concept of a cellular automaton is effectively an expression of the minimum structural and algorithmic requirements of computation but also challenges the idea of processor and memory being separate entities. The computer pioneer Konrad Zuse may not have had this precise interpretation in mind in his seminal 1969 book (Zuse, 1969) as his thesis was that such mechanisms might in fact underlie all of time and space but this is still a reductionist approach and, having effectively given birth to a new sub-field of computer science, it has then certainly been a reverse perspective (i.e. that complex computation can arise through the simulation of cellular automata) that has become the starting point for a wide variety of applications.

A concise definition of what constitutes a cellular automaton is not hard at

this point in history since so many variations exist and have given rise to a very general fundamental description, comprising a declarative part and an imperative part:

Declarative: A data-structure consisting of an array (of any dimension) of cells with each cell able to be in one of a number of states at any given time.

Imperative: A set of rules as to what state a single cell will change to given its current state and the state of it's neighbours (there are several variations as to what constitutes a neighbour but the concept of Higher Order Time Dependence (Ilachinski, 2002) tells us that the one common factor will always be that a neighbour is immediate rather than one or more cells away). These rules are applied to every cell in the array simultaneously at each iteration of the system.

Probably the most famous example of a cellular automaton is Conway's (1970) "Game of Life" which provides a contrived example of cell-colony behaviour. It uses a *Moore neighbourhood* which simply refers to the fact that all cells around the center-cell are considered neighbours (as opposed to the von Neumann neighbourhood which considers only north, south, west and east cells to be neighbours) and the following rules:

> **Birth:** replace a previously dead cell with a live one if exactly 3 of its neighbors are alive.

Death: replace a previously live cell with a dead one if either (1) the living cell

has no more than one live neighbor (i.e. it dies of isolation), or (2) the living cell has more than three neighbors (i.e. it dies of overcrowding).

Survival: retain living cells if they have either 2 or 3 neighbors.

(Ilachinski, 2002b)

Repeated iteration of these rules on a grid with some arbitrary initial configuration results in non-linear behaviour (i.e. behaviour that cannot be modelled by a system of linear equations) and will reliably produce specific patterns which effectively provide the model with its own signature.

Of more relevance to work involving sound is the cellular automaton known as the Greenberg-Hastings model. Originally created to model oscillating chemical reactions, it was adopted in this study as an abstract representation of the propagation of sound-waves and forms the fundamental mathematical core of the work. Its rules consist of two boolean equations representing refraction (R) and diffusion (D):

$$R(\sigma) = \{2 \text{ if } \sigma = 1, \quad \textbf{(2.4)}$$

$$\{0 \text{ else}$$

$$D(\sigma_0, \sigma_1, \sigma_2, \sigma_3, \sigma_4) = \{1 \text{ if } (\sigma_1 = 1 \text{ or } \sigma_2 = 1 \text{ or } \sigma_3 = 1 \text{ or } \sigma_4 = 1) \quad \textbf{(2.5)}$$

$$\text{and } \sigma_0 = 0$$

$$\{0 \text{ else}$$

Combined with the initial state shown, these rules quickly produce patterns of oscillation:

Figure 2.5: Evolution of Greenberg-Hastings cellular automaton

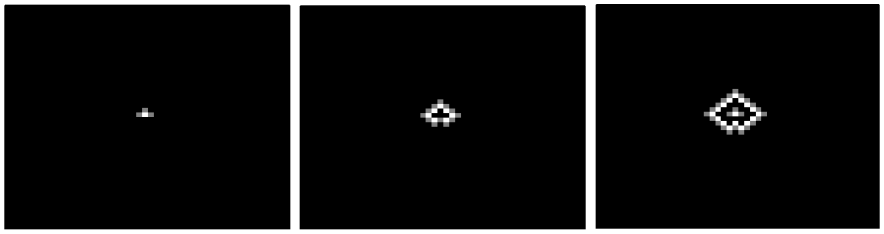

2.8 Microsound

Computer Science is discrete by nature and so it immediately makes sense to look at possible discrete representations of any phenomenon on which one intends to work within the digital domain. Sound waves are continuous in nature and simply choosing an arbitrary way of dividing them up does not take full advantage of what the discrete world has to offer. Of great importance to anyone working with sound using computers is the notion of a sound 'granule'. This concept can be both a physical quantum and a psychoacoustic concept since it represents the minimum length of a piece of a sound wave that can be perceived by the human auditory system as sound. Given the ability of many surgeons to identify the existence of an atherometous plaque in the carotid artery merely by listening to the turbulent blood flow with a stethoscope, it is appropriate to attempt to provide the computer with a

more human means of understanding the physical phenomenon.

2.9 Semiotics

The short definition of semiotics is given by Chandler (2013) as "the study of signs"; the key to understanding the starting point for this branch of philosophy is, however, the definition of 'sign' in that statement. That definition is actually very broad, effectively encompassing any phenomenon that provides us with information. This may be something as intuitively expected as a road-sign or as ethereal as a thought (since having the thought leads us to other thoughts). In the context of medicine, a 'classical' approach is provided by Baer (1988) who discusses the subject from its historical route of symptomatology, the basic premise being that, prior to the existence of diagnostic equipment (in ancient Greece for example), physicians were trained to recognize signs in order to make diagnoses. Baer surveys various semiotics models (formalisations of the process of sign formation and interpretation) that have been developed and then moves on to advocate a reintegration of the psychosocial aspects of medicine into what he considers to be a highly materialist field, modern medicine. This discussion has little benefit to the project described in this thesis however since we are interested in the pragmatics of sign-interpretation in medical imaging. A direct application of semiotic principles to medical-imaging is, however, provided by Cantor (2000) within the field of x-ray interpretation creating a sub-discipline that he has named 'Roentgen Semiotics'. It is

the principles on which this discipline is founded that are of direct relevance to this project.

Despite the absence of X-rays or even of a similar technology in this project, Cantor's work is very useful for the simple reason that it provides a formalisation of the separation of 'visual-absolute' present in a medical image and the diagnosis resulting from examination of that image. In informal terms, Roentgen Semiotics represents all phases of diagnosis by medical imaging in terms of signs and shows how they relate to each. It then becomes possible to replace X-rays with any other kind of medical imaging technology and still find that the sign-relations which were built on top of them apply to the substitution. What makes this possible is the use of the *semeiotic* of Charles S. Peirce.

The perhaps better known philosophy of signs is that of one of the founding-fathers of semiotics, Ferdinand de Saussure, who breaks them down into two components: the sign and the signified. Peirce, however, uses three-components: The *referand* (roughly equivalent to Saussure's sign), the *object* (roughly equivalent to Saussure's signified) and the *interpretant* (no direct equivalent in Saussure's formalism although present in the relationship between sign and signified). The interpretant, as the name suggests, encapsulates the interpretation of the sign by the person observing it and, combined with the inclusion of thoughts themselves as signs, Peirce's system comfortably incorporates the concept of *infinite-semiosis*

where an initial sign, upon being observed, gives rise to the creation of numerous others. It is through this mechanism that Cantor is able to separate the signs of medical diagnosis based upon a medical image from the signs (geometric, topological, etc.) present in the image itself.

It is not useful to this project to go into detail about those aspects of Roentgen Semiotics that are inexorably linked to X-ray images but it is useful to cover the hierarchy of signs that arises from its Peircean analysis.

We will refer to the level of said hierarchy in which the signs discussed are most closely tied to X-ray images as the 'bottom', to whit that this level is based upon the concept of 'Radiographic Boundaries'. These include 'Visual Separation' and 'Visual Contrast'. At the next level up, Cantor abstracts the concept of Visual Separation into either 'Line Separation' or 'Edge Separation' - the former is where a distinct line is perceived, the latter is where the line comes from the existence of an edge (the anatomical equivalent of, for example, the line made by the coast of a land-mass). Visual Contrast is broken up, similarly, into sign-types such as 'Gradient Signs' and 'Density Signs'. Moving up a level we start to talk about the direction of gradients (light-to-dark vs. dark-to-light, etc.) and the appearance and disappearance of signs in general. One level further up finds the inclusion of personal experience and consultation with colleagues in the formation of the interpretant sign during a diagnosis and the new signs (complete with their own interpretants) that arise from this (the infinite-semiosis discussed above). From the point of view of this project,

the usefulness of Cantor's work is that it allows us to say that the output from the system produced to tackle the problem of imaging atherosclerotic plaques is valid in a medical context if it can be placed in substitution for the actual X-rays upon which Roentgen semiotics is based.

2.10 Physical simulation

The collection of data from a real occluded carotid artery is neither practical nor desirable for this project since the aim is to construct a system that can correctly indicate certain distinct topological features. Attempting to do this with a real-life example would introduce difficult ethical requirements and produce data that would be of little use since no control over the plaque topologies involve would be possible. As a result, it is necessary to construct a physical analogue of an occluded carotid artery based upon established material equivalents.

2.10.1 Artificial substitutes for the carotid artery

The use of rubber-tubing to simulate the arterial vessel itself is a long established technique with urethane-rubber being included in a recent review of tissue substitutes for ultrasound imaging (Culjat *et al.*, 2010) and silicone-rubber being demonstrated as a viable substitute by Fatemi (2003) for a detailed study of the vibrational properties of arterial walls with specific reference to non-contact

ultrasound. Whilst this thesis does not deal with ultrasound, Tsangaris and Drikakis (1989) showed that a mathematical model of pulsating blood flow could be created using an anisotropic elastic tube and it therefore seems reasonable to infer that such a material (of which rubber is an example) would be suitable for other acoustic-based work relating to arteries. Since the Young's Moduli and densities of urethane, silicone and natural rubber are close to each other (see table below), we may assume that their acoustic attenuation properties are also similar and that rubber in general is an appropriate material to represent the carotid artery for the problem addressed here.

Type of rubber	**Young's modulus**	**Density**
Urethane	2 to 10 MPa	1250 kg/m^3
Silicone	1 to 5 MPa	1250 kg/m^3
Natural	1 to 5 MPa	910 to 930 kg/m^3

Table 2.1: Comparison of young's moduli and densities for different kinds of rubber (Matbase, 2014)

2.10.2 Artificial substitutes for carotid plaques

Exact physical simulation of the physical properties of a carotid artery plaque is neither required or desirable for this stage of development of an imaging system. Kingstone *et al.* (2013) have demonstrated the use of pieces of Frankfurter sausage to provide something approaching plaque material from soft-plaque up to calcified-plaque, it is only the latter that is relevant to this thesis since until we know

how sensitive the system being developed is to minor variations in topology, we need both the topology and geometry of the simulated plaques to remain constant. It is therefore pointless to take something with a degree of elasticity and strengthen it as opposed to using something that is hard when placed into the simulated artery but can be molded outside of that into whatever form is needed for each experimental run targeting a specific topology. This facility is provided by polymorph thermoplastic which can be formed into any shape once heated to 60 degrees celsius but becomes hard and stable below that.

2.10.3 Artificial substitute for blood

Tsangaris and Drikakis (1989) confirm that blood can be treated as an incompressible fluid for the purposes of physical simulation related to pressure waves. That incompressibility is the most important property to have equivalent between human blood and the chosen substitute is shown in Vendantham and Hunter (1997) who confirm the intuitively correct idea that sound-wave propagation in an incompressible flow will experience advection. The most freely-available incompressible fluid is water: its selection as a substitute for blood here eradicates the need for additional laboratory apparatus (for recirculation of a more specialist fluid) while retaining those characteristics of blood which are significant to the problem of imaging a carotid artery plaque based upon passive acoustic energy.

2.11 Key findings

It is evident from inspection of the phenomenon of sound produced by fluid turbulence and the physical laws that govern it, that the data with which any medical imaging system must work will be nonlinear in nature, not to mention highly prone to noise. The areas of existing knowledge that are therefore most relevant from the review above are those that work with data of a similar nature. Given the very specific form of the phenomenon of turbulent sound it was decided that these would in fact be the two criteria for determining whether or not previous work is worthy of examination in the context of this project. Using these criteria, we can analyse some of the work surveyed from the point of view of how problems similar to those addressed here have been dealt with by others.

2.11.1 MRI and computed tomography

Whilst both of these techniques leverage analytical mathematics in order to perform imaging of the inside the human body, they are both reliant on specialised hardware and directed energy (which the sound emitted from an artery by turbulent blood-flow is not). The Algebraic Reconstruction Technique effectively provides a high-level abstraction of these techniques and might provide a starting point if perhaps combined with some form of regularization (see below) but the matrix used by such a technique would be highly sensitive to changes in the background noise in

its operating environment (a doctors surgery, for instance), nor would the approach be able to deal with the loss of information which Dobashi *et al's* work (2004) indicates is unavoidable.

2.11.2 EIT

From the point of view of this project, it is very reassuring that, given the complexity of the problem, which is close to that to be dealt with in this project, a relatively simple mathematical technique can make the data usable for diagnosis. The technique of Tikhonov Regularization also has mathematical roots of a linear nature which suggests that when working with data of this kind, it may be possible to apply some useful smoothing technique to make it possible to work with less complicated mathematical formulae.

2.11.3 Ultrasound

The principles of Doppler Ultrasound and, in fact, Ultrasound in general are of no major use to this project as they require specialist hardware (transmitter and receiver) and in any case are not ideally suited to the degrees of freedom required of a 3D model of something as small as an arterial plaque in such a way that a surgeon can rotate and translate the model on the screen. This project's approach is to work with what information is inferred by the smallest number of variables possible;

currently just one variable: acoustic pressure. In Doppler-based systems, the sound from inside the artery is reproduced from the beats and could therefore be used as input to the system but this would invalidate the project's requirements of affordability and minimal dependency on specialist hardware.

2.11.4 Kalman filters

There are two distinct problems with the idea of applying a Kalman Filter or variant to the phenomenon of sound produced by fluid-turbulence: Firstly, the technique relies heavily on the probability density functions being Gaussian (Lei *et al.*, 2010), and there is significant research indicating that this is not the case for fluid-turbulence, particularly at a small-scale (Srineevasan and Antonia, 1997). This would result in a lack of stability of the generated matrix during successive update phases of the algorithm. This problem would, in practice, be compounded by the resultant requirement to distribute software relying upon a supplied covariance matrices (which represent information about the errors present) to different environments (GP's surgeries) with different kinds of background noise. The likely effect would be a requirement to have new covariance matrices generated for environments sufficiently divergent from that in which the system was originally calibrated. This would require the presence of the physical artery simulation and a skilled operator. Combined with the non-Gaussianity problem, the practical applicability of such a technique would be severely reduced.

Another variant, the Particle Filter (Gorden *et al.*, 1993) seeks to avoid the problem of non-Gaussianity by adopting a Monte Carlo approach where by multiple model-runs are propagated forward in time until they 'hit' system states produced by the ideal model. In order to properly represent the system state for the phenomenon of turbulent sound generated by an irregular shape (such as a carotid artery plaque), it would, however, be necessary to represent the relationship between the amplitude at a particular point in time and the occupied status of each voxel explicitly thus increasing the dimensionality of the problem. The efficiency of this process is poor, particularly (van Leeuwen, 2011) since multiple model-runs are required for realistic simulation. While van Leeuwen (2011) proposes directing the model-runs towards the measurements for the specific case of geophysical fluid-dynamics, this requires that errors are Gaussian in nature - the very problem that led us to consider Particle Filters in the first place.

2.11.5 Higher-level techniques

Having found no existing medical-imaging work that provides a solid starting-point for this project, a series of higher-level techniques in the form of general approaches to computation and problem solving were surveyed covering areas such as numerical methods, cellular automata and semiotics that provide various abstract perspectives on the different facets of the problem addressed.

2.11.6 Physical simulation

Existing work validates the use of freely available materials for the construction of a physical simulation of an occluded carotid artery. Were more elastic plaque-simulations of interest for this study, it would be necessary to investigate the Frankfurter-based approach described by Kingstone *et al.* (2013) but since that would actually be detrimental to the initial topological investigation being undertaken, polymorph thermoplastic is the best choice.

Chapter Three

Preliminary approaches considered

3.0 Preliminary approaches considered

A lateral-thinking approach permeates this work, driven both by the state of non-linear physics at the project's inception and by a desire to accomplish two, seemingly mutually exclusive benefits to those suffering from carotid atherosclerosis. The result of this is a methodology based upon two levels of abstraction from the specifics of the physical problem. Firstly, regardless of the method(s) eventually used to process the data taken from an artery, it was necessary to be able to create such data in a controlled fashion – specifically in terms of topological and geometric features of the plaques; these are not regular in the real world and thus create a problem for the testing and calibration of any medical imaging system.

In order to maintain as many realistic environmental factors (which is to say, factors that would commonly be present in the device's normal operating environment) whilst retaining practical control of the topological features of the plaques being studied, an apparatus was created for physical simulation of the phenomenon of arterial occlusion. This consisted of a allowing water to flow through a rubber tube at the approximate velocity at which blood flows through a human carotid artery. Occlusions were created by forming polymorph plastic into shapes with distinct topological features and the inserting these 'mock-plaques' into the tubing. The sound of turbulent flow around the occlusion was then recorded via a

microphone inserted into the head of a stethoscope, an arrangement that was proven pragmatically to produce clean and consistent sound whilst not completely damping background noise (thus allowing errors in the data to be dealt with from the outset of the system design).

Figure 3.1a: Physical simulation of occluded artery with stethoscope/microphone assembly to record sound produced by turbulence

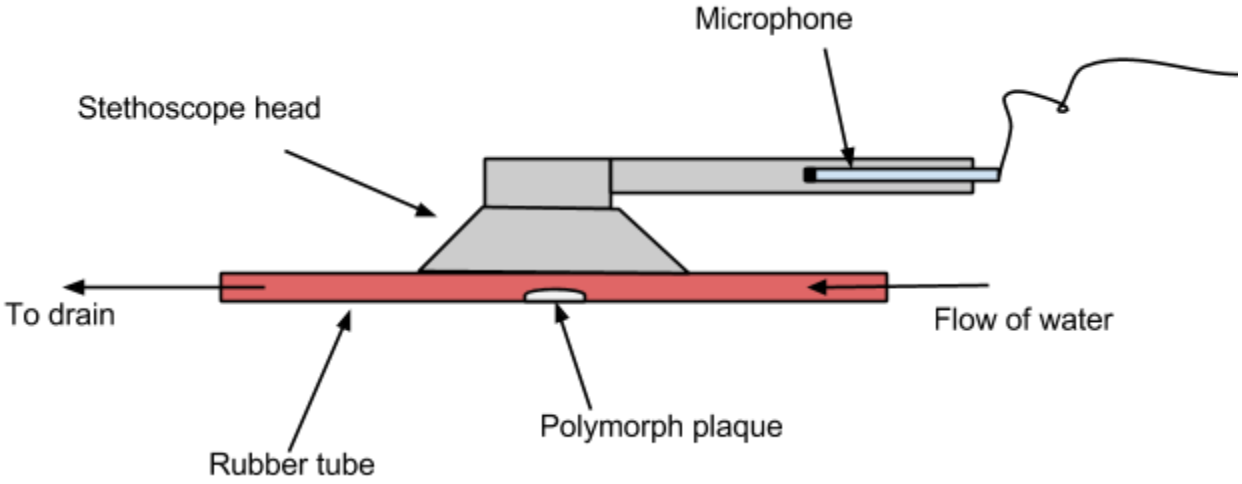

Figure 3.1b: Physical simulation in clamp

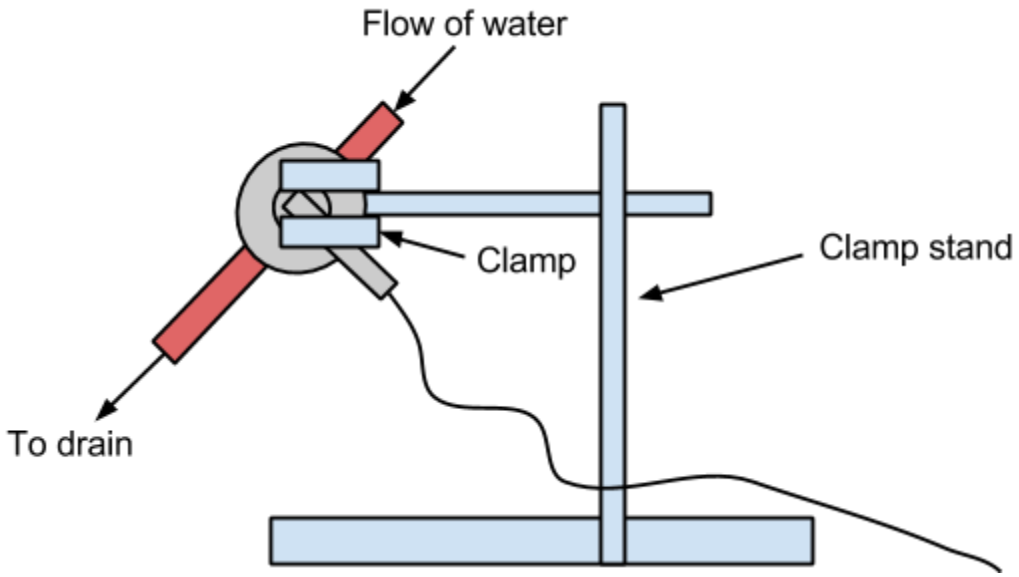

From the point of view of data-processing and the resultant algorithms of the imaging system, our lateral approach called for a three-fold investigation, derived from the semiotic spectrum which results from a digital treatment of non-linear physical data.

In its raw form, the data is a time-series: amplitude values for samples taken at regular intervals in time. The natural assumption then is that an approach designed to work with purely numerical data is the correct one. It rapidly becomes apparent however, that while one might be able to justify with equations the theoretical correctness of a purely numerical approach, the practicalities of implementing it may well turn out to be insurmountable with current technology.

A less obvious but equally pure approach is to attempt to deal with the data

symbolically. This approach is inspired by the dichotomy just described in which it is possible to symbolically prove the theoretical correctness of a technique which is impossible in practical terms. The challenge for this project specifically was how to convert the numerical data coming into a computer into a symbolic form such that strings of numbers became terms of equations. Progress was made towards this end but it quickly became apparent that the amount of work required to mature the technique to a point at which it would be usable was just as prohibitive as the practical obstacles presented by a purely numerical approach.

Given this emergent symmetry of frustration, it then seemed appropriate to attempt a hybrid approach between the two extremes of number and symbol and it is this approach that ultimately resulted in a workable system for extracting and visualising topological information about carotid artery plaques. In taking this 'triangulatory' approach, a spectrum of semiotic reasoning has emerged running from the purely numerical to the purely symbolic, with our solution in the middle and the interaction of these two opposing forces that provided a means to move forward is worthy of elaboration.

Being representable either by mathematical fluid-dynamics or an EPI functional, it can immediately be seen that the problem can be tackled either by calculation or by abstract reasoning, at least theoretically. As far as the actual practicability of these two approaches however, much context can be gained by an

examination of the EPI principle in action in the form in which it is normally used.

The problem with the first approach is the sheer complexity and volume of calculations that must be performed. As will be demonstrated, even a numerical approach based upon a computationally simpler numerical reification of the EPI equation fails to perform adequately for even a simple mathematical problem and it cannot therefore even be hoped that it would handle searching in the far more complex space defined by the mathematics of fluid-turbulence. In the second approach, it quickly becomes apparent that while increased abstraction reduces computational complexity, it does so only from a mechanical standpoint - a payoff is required and, unfortunately, this comes in the form of a greatly increased need for mathematical intuition and creativity - something that no computer currently possesses; artificial intelligence therefore becomes the natural mediating force and a viable approach positions itself in the aforementioned spectrum of semiotic reasoning based upon the balance between how much intuition and creativity artificial intelligence can provide and how much concrete, mechanical computation it must still rely upon. This thesis will therefore define the ends of this spectrum by detailing the two approaches that identified them and then demonstrate the natural emergence of the resultant compromise approach as well as detailing its subsequent development and success.

3.1 Numerical approach

The specific problem addressed by this project can be abstracted to the mathematically equivalent problem of producing a sufficiently accurate approximating polynomial between a vector **x** and a scalar f(**x**). An initial polynomial which will serve as the basis on which to build has been created by evaluating the Lagrange Interpolation formulae within a Geometric Algebra framework thus eliminating the need for the derivation of multivariate versions of the formulae such as those described by Sauer and Xu (1995). The use of Geometric Algebra as a tool for multivariate modelling has since been published by the author (Burley *et al*, 2006).

Having created a mapping between **x** and f(**x**), the next problem addressed is that of improving its accuracy. This seems to be an obvious area of application for the the Frieden-Soffer principle of Extreme Physical Information (Frieden, 2004). This principle involves the minimisation of the differential equation where I is the Fisher Information present in the observation of a physical phenomena and J is the total Fisher Information available about that phenomena (which in real terms can never actually be obtained). The normal approach to applying the EPI principle is an algebraic one: The equation for I is of a fixed form while that for J is determined by the known properties of the phenomena being measured along with an “Invariance Principle” (Frieden, 2004) such as, for example, the continuity of charge and

current-flow in classical electrodynamics . Solving the EPI equation given above then (with a degree of skill) results in the Lagrangian for the phenomena. This is often achieved using the calculus of variations as the formula for Fisher Information is a *functional* rather than a *function*:

$$L(\theta) = E\{[\tfrac{\partial}{\partial\theta} lnf(X,\theta)]^{2}|\theta\} \qquad \textbf{(3.1)}$$

where f is the likelihood function of **X** given some parameter θ and E is the expectation of the formula in curly brackets. In statistical terms, this is the *variance* of the *score*.

In Frieden's work however, the following form of the formula is used:

$$I = \int dx.p'^{2}(x)/p(x) \quad \text{where } p' \equiv dp/dx \text{ and p is the probability of } \mathbf{x} \text{ occurring.} \qquad \textbf{(3.2)}$$

There are two problems with applying this principle in numerical terms: 1) The direct calculation of Fisher information requires knowledge of the probability density function of the phenomena in question – in our case this is difficult to acquire without further approximation and is thus to be avoided if at all possible and 2) We do not have a polynomial representing the total amount of information in the phenomena – if we did, we would not need to further refine our approximating

polynomial in the first place. To illustrate the level of creative problem-solving required to use the EPI principle in the form in which Frieden conceived it, an expanded version of one of his example derivations is provided in Appendix A.

The first problem can be settled by a special case of the Cramer-Rao inequality that relates the Fisher Information to the Squared Error of the phenomena:

$$e^2 I \geq 1 \qquad \textbf{(3.3)}$$

In the case of an *efficient* measurement, this inequality becomes an equality and we can thus define the Fisher Information as the reciprocal of the square error. This approach works for Lagrangian Polynomials being computed and evaluated in a computer because the efficiency of measurement (i.e. of evaluation) is sufficiently near to perfection (with the right programming).

The closest that we can come to the bound-information function from a numerical-analysis perspective is what will be referred to here as a *virtual abstract function* (VAF). The concept is original to this project and consists of defining a function that, while related to the function being optimised (in this case, a Lagrange Polynomial) always has more Fisher information (i.e. a lower squared error).

In order to work with functions and functionals in a concise and efficient form, a survey of geometric algebra techniques and technologies has been conducted to determine whether or not this mathematical structure would give an advantage.

It is widely known that working with vectors, or simply multivariate data sets often requires at some level that the individual coordinates (or data-values) are treated as individual entities. This can result in an increase in the complexity of data-processing systems, especially at design-time resulting in longer development times an increased risk of bugs. In the latter half of the twentieth century, an alternative to vector-algebra began to gain in popularity; Geometric Algebra (or GaL) is Hestenes and Sobczyk's (1984) interpretation of an anti-commutative algebra developed by the noted mathematicians William Kingdom Clifford and Hermann Grassman. Whilst Geometric Algebra is of interest in a number of areas of pure mathematics, from the point of view of this project, the potential benefits resulting from the unification of scalars, vectors, complex numbers and quaternions are apparent.

3.1.1 A Genetic Algorithm over Geometric Algebra

It is at this point that the advantage of using Geometric Algebra within the theory of vortex sound becomes apparent: In many cases, the virtual abstract function

may be defined as the magnitude of **x** mapped to f(**x**) (which is scalar already for the vortex sound formula which the system to approximate). Geometric Algebra allows us to express both the virtual abstract function and the polynomial being optimised using the same entities (called pseudoscalars) thus making minimisation of the Fisher Information differential a straightforward problem that can be solved using a simple genetic algorithm or any other algorithm that can search through a given domain (Hooke-Jeeves, Nelder-Meade, etc.). The solution of the differential equation is a function g(**y**) (the system does not actually give us the values of **y** but it seems sensible to refer to g as a function as continuity is implied by the simple fact that our choice of data points in $G_{3,1}$ is arbitrary) which it is hoped can be used to optimise the approximating polynomial.

Figure 3.2: Graph of solution function g(**y**).

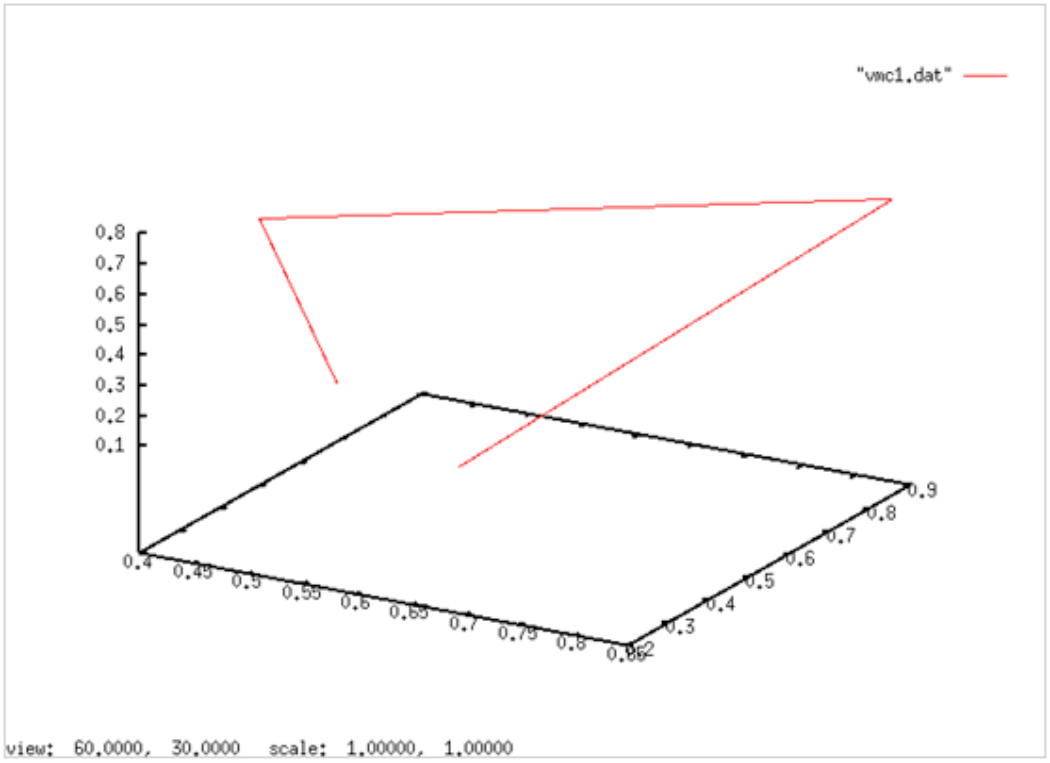

A genetic-algorithm based implementation of this technique has been tested for the problem of computing vector-magnitudes. This problem is simpler than the main aim of the project but has an identical functional definition (i.e. mapping a three-dimensional vector to a scalar). The results of the genetic algorithm suggest that the solution function g(**y**) is always significantly non-linear (graph 5.1). This may hold a clue as to the form of the more accurate approximating function as the condition required for computing the original Lagrangian Polynomial is that the input values must be equally space and therefore must lie along a single vector. The solutions to the Fisher Information differential for the vector-magnitude problem are, so far, always non-linear. This suggests that the next stage of the process would be to use another genetic algorithm to alter the coefficients of the polynomial in order to

allow the solution of the differential equation to meet the linearity condition of the Lagrange formula when re-expressed using Geometric Algebra. A corollary of this is that we can now define the accuracy of a Lagrangian interpolating polynomial as the curl of the solution function, i.e.: although this is not directly computable at the present time.

In effect then, what this initial work suggests is that a numerical implementation of the EPI principle can be created and geared towards the derivation of a Lagrangian that relates the space occupied by an atherosclerotic plaque with the change in sound pressure at time t caused by the turbulence of blood flowing over and around the said plaque

3.1.1.1 Architecture of Genetic Algorithm

The genetic algorithm has been implemented as an object-oriented program in the Java programming language. The classes (modules from which any number of usable instances can be created) are as follows:

Monad,

MonadPatch,

DataPoint,

LagrangePolynomial,

FisherInformationDifferential,

SolutionFunction,

MainAlgorithm.

Monad provides an implementation of Geometric Algebra for three geometric dimensions (resulting in eight linear dimensions). This is part of the Clados library. A Monad can be thought of as a pseudoscalar although in implementational terms it also contains methods for performing arithmetic on pseudoscalars.

MonadPatch corrects a fault in the .clone() method of the Monad class.

DataPoint represents a pair of Monads.

LagrangePolynomial represents a Lagrangian Interpolating Polynomial. Supplied with an array of DataPoints at instantiation, LagrangePolynomial objects automatically compute their coefficients based upon this array. They can be instructed to differentiate themselves as well as clone.

FisherInformationDifferential stores two LagrangePolynomial objects (one representing the VAF and the other representing the polynomial to be optimised). A FisherInformationDifferential object can be asked to evaluate itself and this is in fact

exactly how the MainAlgorithm class implements population-evaluation.

SolutionFunction represents an array of Monads that can be asked to mutate itself as well as undertake crossover with another SolutionFunction. It is the programs implementation of the chromosome concept.

MainAlgorithm is the program's entry-point. The methods in this class handle loading of data and output of solution-functions along with displaying the majority of console messages used by the program. It initialises the pool of SolutionFunctions and performs the evaluation (by calling a method in the FisherInformationDifferential class) of that pool (the population in genetic algorithm terminology). The fitness function for an individual chromosome is simply the result of evaluating the FisherInformationDifferential for that chromosome. Two approaches to minimisation of the differential have been tried, the most obvious being to solve it for the value 0. In reality, the number of calculations that have to be performed in order to do this result in unacceptable inaccuracies arising in the results. This is in part due to the tendency of the VAF to have only slightly more

Fisher Information than the polynomial being optimised. This is acceptable for this project and will only need to be improved upon if using the approach of solving the derivative for f'(x) = 0 becomes vital. To avoid this problem at the moment, the algorithm simply searches for a solution that makes I - J as close to 0 as

possible. This is justified by the fact that the extremum of I - J being anything other than 0 would mean that the measuring instrument (the approximating polynomial) was either necessarily inaccurate, an absurd statement, or that it could in fact acquire more information about the phenomenon being studied than the phenomenon itself contained, suggesting that either the phenomenon or the approximating polynomial were counterfactual. The selection technique currently being used is Tournament Selection which tries to ensure that selection pressure is kept constant (Mitchell, 1998) thus avoiding premature convergence on a sub-optimal solution.

3.1.1.2 Issues with the approach

3.1.2.2.1 Conceptual

As has already been stated, the definition of Fisher Information used in this project will be based upon the Cramer-Rao inequality which specifies a lower bound for the relationship between Fisher Information and Squared Error. This means that, because of the Root Mean Square calculation used to compute e^2, the dependency of the Fisher Information upon the order of data-points seems to be lost (as addition is associative). The fact is however that the Cramer-Rao inequality *can* be used in this way (and is in fact used like this in Frieden's EPI derviation of the law of 1/f noise); it simply specifies that the lower-bound for the efficiency of measurement/estimation

has been achieved. This raises an interesting question about the use of Fisher Information (in the form used by Frieden) over Shannon Entropy in situations where efficiency is 100% (or a negligible distance from 100%).

3.1.2.2.2 Regarding current implementation

In applying the numerical EPI technique as it currently is to the problem of producing a Lagrange Polynomial for approximating vector-magnitude, it will be apparent that the virtual abstract function (which maps the magnitude of the input pseudoscalar to the magnitude of the output pseudoscalar) is actually of the form $r(|\mathbf{x}|) = |\mathbf{x}|$. This meets the condition that the VAF has more Fisher Information than the initial approximating polynomial but a question arises as to whether or not it's form is a suitable 'scalar analogue' to that polynomial. Reassurance can be found on this by an application of the symbolic EPI technique to the problem of price fluctuation in Econophysics (Hawkins and Frieden, 2004). In this application, the bound information J is actually defined as 0 resulting in the EPI equation reducing to simple minimisation of I. The approach successfully derives the Lagrangian sought and so the argument used in this project for equivalent cases (such as vector-magnitude approximation) will be that the validity of such a choice is context-dependent. It would however be necessary to demonstrate this with applications to different kinds of problem. These would range from simple, abstract

problems such as the vector-magnitude calculation described above, through the production of Lagrangians for actual physical phenomena. As well as helping to fine-tune the technique, this would result in publishable work in the fields to which the technique is applied and the act of fine-tuning would therefore have numerous corollaries for those fields.

3.1.2.2.3 Exacerbation of premature convergence

Unfortunately, the VAF concept doesn't take the search in the same direction within the vector space of possible solutions that the bound-information would (if it were possible to numerically express the bound-information). Speaking in terms of Peircean semiotics, the problem stems from switching from object to referand and thereby producing a subjective result for an objective problem. Even infinite semiosis will not work as the process will go further and further into the interpretant.

One way around this might be to create several different VAFs with the hope of identifying the centroid of the range described by the different outputs from the algorithm. This might prove a hard problem in itself, since each VAF could potentially introduce new ways for the algorithm to converge on a sub-optimal solution (also known as 'premature convergence' (Mitchell, 1998)). Even after these difficulties were overcome (assuming they could be), it is still possible that the

centroid would not be of use as a solution to the EPI equation.

Given that there is a potential to expend a great deal of time and effort on this approach with no guarantee of a usable result, it was decided at this point to pursue a more abstract approach.

3.2 Symbolic approach

3.2.1 Computational approach

Given that the EPI problem appears to implicitly require a symbolic algebraic or, impossibly as it turns out, a numerical solution it seems at first glance that any methodology attempting to address a phenomenon via Fisher's approach in a computational ('computational' having a strong synergy with 'concrete' in this context) way must ultimately hit a dead end. This is because physics, mathematics and most other sciences make an absolute delineation between symbolic (as in algebraic manipulation) and numeric (as in calculation). This delineation is in fact an illusion but the work which illustrates this is not widely known about; the reasons for this are speculative and are therefore not appropriate for discussion in this thesis; we will instead simply proceed to demonstrate a symbolic/numeric fusion through the construction of a formal system interpretable from either viewpoint.

The starting point for the construction is the concept of a Virtual Abstract Function (VAF) developed in the previous, purely numerical approach. The VAF is intended to satisfy the requirement of bound-information function, J, by numerically modelling as much macroscopic behaviour of the information associated with the phenomenon in question. This approach is justifiable if we consider the bound-information to be a preliminary experiment in determining the overall physical behaviour of the phenomenon. We can express this mathematically using Jumarie's (1990) notion of conditional entropy.

3.2.2 Using conditional entropy to investigate a definition of the bound-information J

The validity of the VAF concept can be investigated in part by the techniques of Jumarie (1990) who provides a formal derivation of the conditions that must be met by a supplementary experiment in order to completely define the primary experiment. In the case of the EPI method as applied to the research question, the primary experiment is the derivation of a physical law relating features of a carotid artery plaque to the sound produced by turbulence in the blood-flow around it (represented in the numerical system by an initial approximation in the form of a Lagrangian interpolating polynomial), and the supplementary experiment is the

Virtual Abstract Function. Using Jumarie's notation, we have the primary as β and the supplementary as α. In order for α to completely define β, the conditional entropy H(β/α) of β given α must be zero. It is possible to show that this results in the following inequality regarding the individual entropies of the two experiments (Jumarie, 1990): $H(\alpha) \geq H(\beta)$. In our case, it is therefore necessary that that VAF brings at least as much information as the initial approximation. It seems reasonable that this should be the case as the Lagrangian interpolating polynomial will contain features that are not present in the phenomenon being measured whereas the VAF will contain only a subset of those features.

3.2.3 Results of the entropic investigation

The conditional entropy function effectively acts as a conduit through which information can flow between the primary and supplementary experiments. It is worth bearing in mind, however, that as well as having a mathematical definition, a complete definition of the information of any part of a system is still subject to relativity. This can be illustrated by taking another of Jumarie's approaches:

If β/α is the amount of information brought by α about β, then β/α/R is the amount of information brought by α about β from the point of view of an observer R. In the numerical EPI solver, R would be the computer program that performs the

minimisation of the EPI functional. The conditional entropy can be extended in the other direction by defining β'/(β/α)/R as the amount of information brought by experiment β about the 'universe' in which it exists when supported by experiment α and from the point of view of the observer R. This poses a problem in that in our case, R cannot have knowledge of β' as this would assume that we already have an exact, objective physical law representing the phenomenon being measured, something that we do not have and that it is most likely not possible to have due to the observer effect. What this means for the numerical approach to the EPI process is that the system can only be guaranteed to minimise the information loss between the initial approximation and the VAF and that there will come a point in the minimisation of the EPI functional where the solution functions generated are being optimised to describe the structure of β rather than β'. This point is not identifiable as it would require the amount of knowledge about β' that is actually being sought by the EPI process and so the numerical approach is infeasible in this form.

3.2.4 Combinators as a bridge between the symbolic and numerical domains

Attempting to use automatic algebraic solvers is out of the question due to the amount of mathematical creativity displayed in most EPI derivations; this represents an absolute boundary (henceforth to be referred to as the *symbolic boundary*). It has also been shown that a purely numerical approach is not feasible due to the effects of

relativity and the observer effect. The key to solving this problem is to find a VAF that can be evaluated implicitly, i.e. in the way such a function is 'evaluated' by being incorporated into the EPI process as it is currently established but that will allow a symbolic solution to be computed easily using numerical-method/AI algorithms.

The theory of combinators provides a solution in this respect as combinators are simple enough to be processed by machine with minimal computational expense and yet can represent complex mathematical entities if sufficient memory is available. In this approach, there are generally a small number of operators (often no more than three) that are applied to each other and can thus also represent values and the need for variables. The initial work of Schoenfinkel (1924), Curry (1958) and, later, Church (1941) all demonstrate ways in which such forms can be defined and manipulated, however the somewhat controversial "Calculus of Indications" of Spencer-Brown (1972) and the following calculus of "Spatial Forms" of James (1993) (see Fig. 5) is more directly relevant to this project as they combine semantic richness with minimal theory. In particular, the calculus created by the latter defines logarithms, exponentials and derivatives which could serve to define a boundary-notation-equivalent of the Fisher Information.

Table 3.1: Some examples of James' boundary notation.

Standard	**Boundary**
1 + 1 = 2	oo = oo
21 + 11 = 32	([b][oo])o([b][o])o = ([b][ooo])o
x * 1 = x	([x][o]) = x
x * 0 = 0	([x][]) =
x^1 = x	(([[x]][o])) = x
x^0 = 1	(([[x]][])) = o
1/x = x^-1	(<[x]>) = (([[x]][<o>]))

Using this approach, all of the entities required for the EPI process can be defined thus allowing the minimisation to be performed symbolically but with symbols that also represent values in a nominal way (as opposed to variables where there is no innate connection between symbol and value except that defined by the user). The only remaining task will be to extend such a representation so that it is able to represent pseudoscalars, something that can most likely be achieved by modifying the 'base' combinator used to represent numbers above 9 (see the second example in Fig. 6.5).

3.2.5 Choice of VAF

Given a pseudo-discrete representation, it should then be possible to choose a VAF that is innately continuous. For a research question rooted in the field of fluid-dynamics, the appropriate construct is a cellular automaton (CA). Put simply, it is possible to model a fluid using discrete, logical rules to generate behaviour at the microscopic level and to then extrapolate macroscopic behaviour from this that agrees with the Navier-Stokes equations as long as we obey the condition that we work within a symmetry group of order 6 (i.e. a the model must operate on a hexagonal grid). The resultant model is known as a Lattice Gas and there are many variations on the basic square-grid model of Hardy *et al.* (1973) which started the research in this area. It turns out that even with a 'traditionally' numerical approach to the EPI process such a model could still have been used but would have then led to an application of the Inverse Ultradiscretization method of Nobe *et al* (2001). This would have introduced a degree of 'smearing' between cells, something avoided by the combinatory-based approach discussed here which merely requires that we re-express the CA's logical rules in a different notation.

Given the functional nature of such a representation, it makes sense to perform the initial implementation of the CA model in a functional language and, given that there is also a need for array-processing, the APL language is most suitable for this purpose. Figure 6.2 shows the terseness introduced; this property of

APL is often considered a bad thing in the programming community but for the purposes of this project, it provides expressions that are closer to being in boundary-form than their equivalents in a less-terse language.

Figure 3.4: APL code for processing particle-collisions for every cell in the lattice (note the lack of explicitly coded loops).

```
t←m=5
n[2;;]←n[2;;]+(1⌽1⌽2×t[1;;])+8×t[1;;]
n[1;;]←n[1;;]+(2×t[2;;])+¯1⌽¯1⌽8×t[2;;]

n[2;;]←n[2;;]-(1⌽1×t[1;;])-(1⌽¯4×t[1;;])
n[1;;]←n[1;;]-(¯1⌽t[2;;])-(¯1⌽¯4×t[2;;])

t←m=10
n[2;;]←n[2;;]+(1⌽1×t[1;;])+1⌽4×t[1;;]
n[1;;]←n[1;;]+(¯1⌽1×t[2;;])+¯1⌽4×t[2;;]

n[2;;]←n[2;;]-(1⌽1⌽2×t[1;;])-(¯8×t[1;;])
n[1;;]←n[1;;]-(2×t[2;;])-(¯1⌽¯1⌽¯8×t[2;;])
m←n
```

The last issue that must be resolved within the new representational framework is that of the data information I. This takes a fixed form in Frieden's symbolic EPI process and has been given the form of an initial approximation in our original numerical implementation. In the combinator-based representation, it can in fact take either and the best choice from these two possibilities would require experimentation to identify. The polynomial representation has, however, already been shown to have advantages over the 'fixed integral' representation as, having been initialised using the data for which the derivation of a physical law is required, it may reduce the computation time required to solve the EPI equations when compared to the alternative. The question thus arises as to whether or not this

approach really differs from a numerical approach using the normal place-value number system as a representation. The answer to this is subtle but important: with a combinator-based representation, it would be possible to examine the evolving structure of the numerical solution to the EPI equation in a way which would require detailed number-theoretic investigation otherwise.

3.2.6 A formal system for representing and solving the EPI process

3.2.6.1 Clifford Algebras

It has been shown (Burley *et al.* 2006) that the Geometric Algebra of Hestenes and Sobczyk (1987) can be used to extend univariate numerical techniques to multivariate domains. The construction of a formal system can therefore begin with the derivation of a qualitative value-system based upon the geometric product so that qualitative analogues of numerical techniques can be created. The linear basis-elements generated by the geometric product of the basis-vectors e^1 and e^2 provide a useful direction for when combined with a holistic approach to science in general. Such an approach that, conveniently, is well rooted in scientific information theory is the *generalised Mendelevian Periodic Table*.

3.2.6.2 Generalised Mendelevian Periodic Table

Haskell *et al.* (1972) generalised the well-known periodic table of the elements using General Systems Theory (Bertallanffy, 1969) such that a non-Cartesian coordinate system representing the cybernetic feedback loop between work-factors and controller was developed. This coordinate system allows particular instances of this cybernetic concept to be assigned to one of three categories of order: Entropic, Ectropic and Atropic. By associating each of these categories with the qualitative results of the geometric product, it can be treated as a feedback system between two qualitative vectors resulting in either an increase or decrease in ectropy/entropy or an atropic situation (neither ectropic nor entropic). Rotating the periodic coordinate system through 45 degrees and applying a similar approach to these three possible products then results in a seven-valued logic (although derivations involving the value Z (see below) are trivial) which allows spatial direction and information (i.e. ectropy, entropy or atropy) to interact with each other as well as providing a useful combinatorial syntax for expressing qualitative vectorial calculations.

We have based our system on a geometric algebra in two geometric dimensions. This results in four linear dimensions and provides the following useful mapping:

Table 3.2: Qualitative multi-vectors and their entropic associations.

Four-dimensional tuple	Entropic association
(0, 0, 0, 0)	Z
(*, 0, 0, 0)	Entropic (N)
(0, 0, 0, *)	Ectropic (K)
(*, 0, 0, *)	Atropic (A)
(*, *, *, *)	Atropic (A)
(*, 0, *, *)	Atropic (A)
(*, *, 0, *)	Atropic (A)

Tuples containing only non-zero values in the second and third positions are not categorised as they represent the initial values of the system.

3.2.6.3 A qualitative evaluation of the geometric product

Table 3.3 shows the result of calculating the geometric product when the coefficients of the three geometric basis vectors are taken from the set of possible values provided by the Qualitative Physics of de Kleer and Brown (1984), namely (-, 0, +). This provides an expanded set of values in which there are, in addition to signed initial values, the hyper-complex values that result.

Our previous work with Lagrange Interpolation over the geometric algebra $G_{3,1}$ (the geometric algebra in three geometric dimensions over the reals) has suggested that in computations involving this algebra, the coefficients of the hyper-complex basis-vectors can provide information about the internal workings of the calculation not available in any of the traditional algebras used for similar purposes. This induces the hypothesis that such values can be sensibly categorised by a periodic coordinate system such that those values containing non-zero coefficients for one or more hyper-complex basis-vectors can be considered to be ectropic in relation to those that do not. The current logical system derived from these ideas is based on $G_{2,1}$ and therefore there is only one higher-ranking basis-element. This provides the neat categorisation given above.

In order to ascertain whether or not the required formal system (which will henceforth be referred to as GEL for Geo-entropic Logic) is constructible, the set of qualitative initial vectors is reduced to the set (0, *) where '*' represents a non-zero value, i.e. if Q represents the set of values (-, 0, +) used by de Kleer and Brown, GEL is built upon the distinct values of the set |Q|. Negative values are not included and any negative values that result in either the rank-0 or rank-3 elements of tuples resulting from the geometric product of the initial vectors are made positive. This is justified on the grounds that, for our interpretation of the three categories of order given above, the tuples (0, 0, 0, -1) and (0, 0, 0, 1) should both be considered ectropic as they both contain a non-zero value in their rank-3 elements and the

difference in sign is a relative issue caused by the anti-commutativity of the geometric product.

Table 3.3: Qualitative Geometric Product Results.

Equation	**Result**
(0, *) (0, *)	(*, 0, 0, 0)
(0, *) (*, 0)	(0, *) (*, 0)
(0, *) (*, *)	(*, 0, 0, *)
(*, 0) (*, *)	(*, 0, 0, *)
(*, *) (*, *)	(*, 0, 0, 0)

3.2.6.4 Derivation of combinators

3.2.6.4.1 Projection, Union and Perpendicular Projection Combinators

We can derive a graphical representation of Table.2 by using the periodic coordinate system. T represents (0, *), C represents (*, 0) and B represents (*, *). We can reduce the geometric product involving any combination of these initial vectors to a sequence of combinators. The first four of these map a vector from one axis to any axis perpendicular to it. They operate as follows:

Projection ($\prod$): Maps a vector to its complement so T maps to C and C maps to T. B maps to (0, 0) but that result prevents any further operations and is therefore disallowed in this system.

Projection over the Axis of Atropy ($\prod_a$): Maps a vector to one which will result in an atropic geometric product. In practice, this means that T and C map to B and B maps to. This last mapping is ambiguous; in some cases, a choice of either T or C will need to be made in order to continue with any further operations, in other cases a choice is not necessary and in fact one can work with a superposition/undefined-state. In practice however, it is not desirable to have such a level of vagueness and in the next section, we describe a derivation calculus which resolves such ambiguities in a paraconsistent way.

Union ($\bigcup$): Maps a vector to the same vector so T maps to T, C maps to C and B maps to B.

Union over the Axis of Atropy ($\bigcup_a$): Same behaviour as Projection over Atropy.

Figure 3.5: Projection and Union combinators.

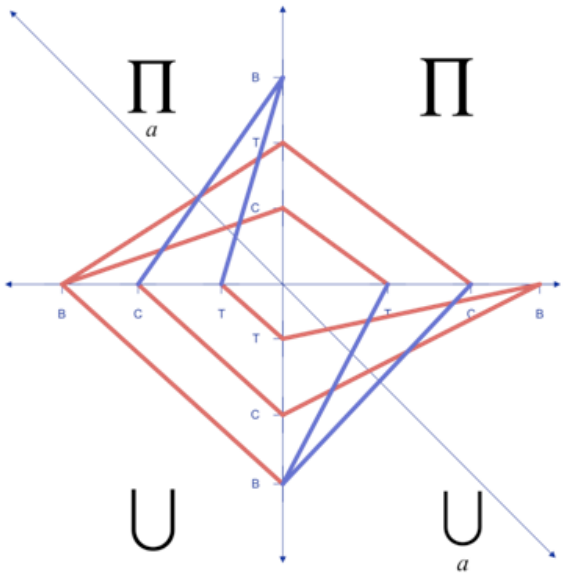

The use of any of these fours operators results in a line begin drawn from one axis to another that is perpendicular to it. Despite the appearance of the diagram in Figure 6.3, the order in which the initial values T, C and B appear on the axes is irrelevant; the coordinate system is non-Cartesian and it is helpful (but not vital) to assume that any line drawn by the application of one of the above combinators will, in reality, have acute angles with its axes of 45 degrees. This assumption is particularly useful in visualising the operation of the next combinatory.

Perpendicular projection (π): Maps one of the values T, C or B to one of the values N, K or A. Behaves the same in each of the four quadrants.

The easiest way to visualise the Perpendicular project combinatory is to visualise the drawing of a line from the point resulting from a projection or union to

the point given by taking the values on whichever of the two axes concerned as coordinates the refer to a specific point in the quadrant demarcated by those axes.

Examples:

1. Beginning with T on the right-hand horizontal axis, is applied. This produces C on the upper vertical axis. is then applied, giving K as a result.

2. Beginning with T on the lower vertical axis of the second diagram, is applied. This produces T on the left-hand horizontal axis. is then applied, giving N as a result.

3.2.6.4.2 Rotated combinators

The irrelevance of the distance along an axis at which an initial value is placed allows us to provide a means of applying the combinators described above to the values which they generate. If the periodic coordinate system is rotated clockwise through 45 degrees and the angle of viewing is then adjusted by the same amount anti-clockwise, we will see an axis-system such as that in Figure 6.4. In this diagram the K on the upward pointing axis represents the K value assigned to the first quadrant of diagram 1. Similar mappings apply for the other axes and quadrants.

Figure 3.6: Rotated periodic-coordinate system.

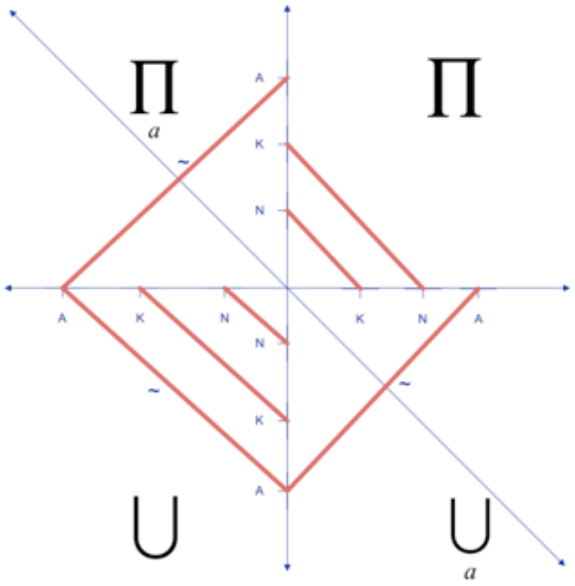

Having created this second axis-system, it is then necessary to define the operations of the combinators for it as producing a new set of combinators would move GEL(|Q|) as a whole towards triviality. This is done in the same way as for the first diagram and results in the relationships shown on the second with the slight difference in that the definition of A as being any tuple that is not (1, 0, 0, 0) or (0, 0, 0, 1) results in ambiguous behaviour for the three combinators that deal with it. Given that there are also ambiguous mappings between T, C and B on the first diagram, it is necessary to adjust the system to deal with these. In fact, GEL(|Q|) itself is left intact and instead a calculus is defined with which to generate derivations/proofs in the system.

3.2.6.5 A calculus for GEL(|Q|)

In order to make derivations/proofs in GEL(|Q|) it is occasionally necessary to express combinations of values (such as) and also to state when something is not the case. It will eventually be shown here that GEL(|Q|) can express Boolean-style equations in the form of if-then-else structures and so it is possible to use the system to define its own calculus. This is unnecessary however since the manner by which a derivation or proof is produced in GEL(|Q|) is irrelevant as long as it *can* be produced. It is therefore easier to define the calculus using elements of Classical Logic. There is however the issue of the ambiguities that can occur in GEL(|Q|) derivations; to solve this problem ideas are adopted from the field of Paraconistent Logic. A modified Fitch-style approach to displaying our derivations/proofs is adopted in order to be able to indicate 'events' that affect the direction taken through GEL(|Q|)'s axis-systems.

3.3.6.5.1 Paraconsistent Logic

The issue of creating a formal system which can deal with inconsistency has been tackled before by numerous authors. The approaches range from using multiple truth values (da Costa *et al.* 2007) to disallowing certain axioms from Classical Logic (Henceforth to be referred to as CL). Given however the specific tendency of some operations in GEL(|Q|) to produce several possible results, the work of

(Vanackere 2000) on adaptive logic seemed most applicable and is in fact the source of the ideas used to resolve such ambiguous behaviour in the system we described here. The mechanism resulting from the adoption of these ideas is best illustrated with an example.

3.3.6.5.2 Some “laws” derived from the system

GEL(|Q|) is intended to unify information along with direction and logic; an argument in support of its ability to do this is the fact that the informational aspect of the system has certain properties in common with Fisher information which is a unifying concept throughout this thesis. This commonality can be shown by following the derivations from an ordered state (K) to a disordered state (N) and vice-versa:

3.3.6.5.3 Transition from K to N

The transition from K to N proceeds as illustrated in Fig. 3.7 (The annotation CDN stands for ConDitioN).

Figure 3.7: Transition from K to N

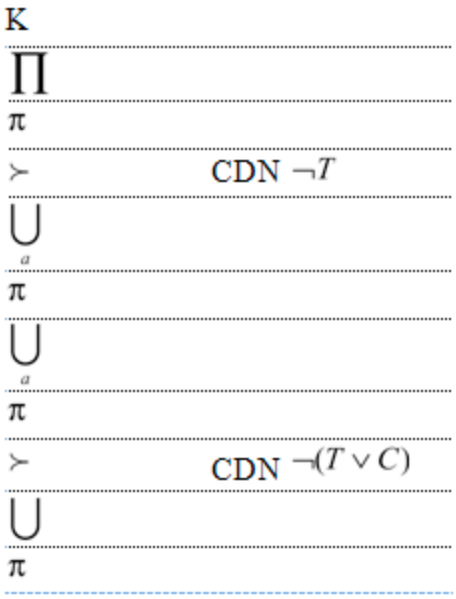

In this transition, we make two contractions and in doing so introduce the possibility that the value we contract to may not actually be the correct one. To indicate this, we make an entry in the second column stating that the value produced by the contraction is only correct if it doesn't turn out to be one of the other possibilities. In this particular case, we find that the conditions hold and thus the result (N) is said to be *finally derivable*.

3.3.6.5.4 Transition from N to K

Figure 3.8: Transition from N to K (The additional annotations stand for (Cannot Proceed and CHoose)).

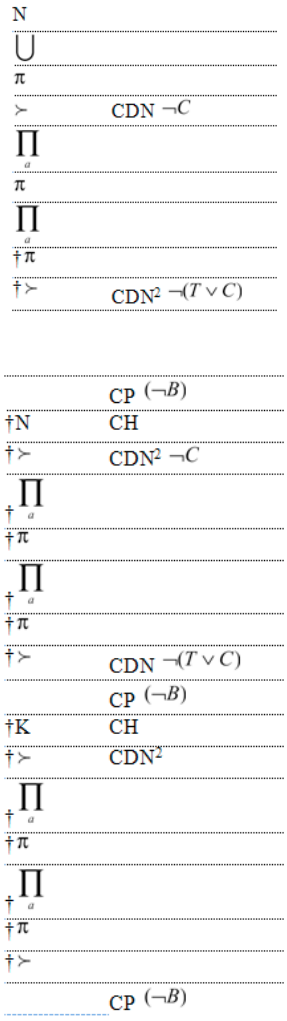

At this point in the derivation it can be seen that, regardless of corrections made based upon conditions becoming negative, it is not in fact possible to find a way of proceeding from N to K. This seems intuitively correct: It is not possible to

proceed from a disordered state to an ordered one without some kind of outside interference which GEL(|Q|) is quite rightly closed to given that it is intended for application to a physical problem. As far as the calculus itself is concerned, if a CP situation is encountered, a backtrack is performed to the condition that has been negated and one of the other values from that condition is chosen as an alternative (assuming there are any available). Derivation/proof then proceeds with the new value once all lines derived based upon the choice that resulted in the CP situation are marked so that they are no longer considered part of the process.

3.2.6.6 Relation to existing information metrics

The last remark in the previous section might seem strange when considered from the point of view of the better-known Shannon Entropy metric used in scientific information theory, given that the amount of Shannon Entropy increases with time. It is thus clear that the information dealt with by GEL(|Q|) cannot be Shannon Entropy given the 'laws' discovered above. Fisher Information, like Shannon Entropy is additive but differs both in the temporal way already described and in that it is locally dependent on the structure of the probability density function for the phenomenon to which it is being described as it contains a squared gradient term.

Given the conceptual similarities between the information present in GEL(|Q|) and Fisher Information, it seems reasonable to now define an information metric for the system. This metric is discrete in nature given the high-level of

discretisation in the system and appears to be able to facilitate the architecture for an symbolic/numeric hybrid automated EPI process already described.

I_Q = (sum(values in ectropic quadrant) – sum(values in entropic quadrant)) / sum(values in atropic quadrants) + 1 **(3.4)**

Thus the information value of a particular derivation is acquired by counting the number of occurrences of N, K and A in that derivation and then using the formula above.

This metric is not an exact discrete equivalent of Fisher's information, but it shares the properties of additivity and negative first derivative, the latter property being effectively built into the system. It is interesting to note that this property arises from the structure of the qualitative geometric algebra. Whilst not a proof, this does suggest that our assignment of ectropy, atropy and entropy to the qualitative geometric product results is appropriate.

In the derivations between N and K given above, the first has $I_Q = -0.25$ whilst the second has $I_Q = -0.67$ (because we cannot count N, K and A occurrences resulting from lines which were marked as a result of a condition not holding).

3.2.7 Arithmetic in GEL(|Q|)

Given that all of the values that can possibly occur when using GEL(|Q|) are already present in its definition, it is found that the operations of arithmetic can be reduced purely to sequences of the existing combinators. The general approach is to choose a combinator that maps the first value to the second value and then to proceed from there using one of the following formulae dependent upon which operation is required. In each formula, 'x' represents any value in GEL(|Q|) and the formulas themselves are given as right-associative strings of combinators to save space.

3.2.7.1 Multiplication

The assigning of K to the tuple (0, 0, 0, *) and N to the tuple (*, 0, 0, 0) effectively split the two terms of the geometric product into two separate products: the dot-product and the wedge-product. These can be represented by GEL(|Q|) as follows:

Dot-product giving non-zero result: $\pi \bigcup x$ **(3.5)**

Wedge-product giving non-zero result: $\pi \prod x$ **(3.6)**

3.2.7.2 Addition

Add a value to itself: $\bigcup x$ **(3.7)**

Add a value to its complement: $\prod_{a} x$ or $\bigcup_{a} x$ **(3.8)**

3.2.7.3 Division

In GEL(|Q|) the modulus-qualitative value set makes division identical to multiplication.

3.2.7.4 Subtraction

The relationship between multiplication and division also applies to addition and subtraction.

3.3.7.5 Boolean logic operators in GEL(|Q|)

It is desirable for GELs to have the ability to express Boolean logic

operations as this would allow the reasoning performed by computer programs to be implemented and thus unified in such a way that it could then be intermixed with reasoning about vectors and/or entropy. This provides an extremely powerful system in which the EPI process could utilise computer programs as bound-information representations rather than discretised mathematical equations. In GEL(|Q|) however there is an obstacle to this in that it has no direct equivalent of True and False. In attempting to overcome this problem, various approaches were tried. A complete interpretation, largely inspired by Kleene's Ternary Logic, of all of the possible combinations of GEL(|Q|) values under the operations of AND and OR was produced and then rendered in GEL(|Q|) combinators to try to identify any general approaches to these operations in the system but, unsurprisingly, the only generality that emerged was that based on homogeneity versus heterogeneity and did not allow the prediction of, for example, any Boolean operation with GEL(|Q|) values in terms of what the correct combinatorial expression would be.

The second approach was to investigate the system to see if it contained one of the sole sufficient operators from which all other logical operations can be constructed. Unfortunately, the only operation that the system came close to modelling convincingly was XNOR and even this required the introduction of a new value, Z, located at the origin of the periodic coordinate system and mapping to itself under all GEL operations.

The third approach (and the one since adopted) was to define the sole-sufficient operator NAND in terms of an if-then-else structure. This can be done as long as the input values come from the set (T, C, B) (such that T v C represents True and B represents false) and the output values come from the set (N, K) such that N represents a negative outcome (intuitive analogy of falsehood with an increase in disorder) and K represents a positive outcome (intuitive analogy of truth with an increase in order). This allows the expression of the AND operation as follows:

$$\pi \prod x \qquad \textbf{(3.9)}$$

$$\pi \bigcup x \qquad \textbf{(3.10)}$$

Where x is the first parameter of the AND operator, and the second is determined by location of a transition from one axis to another, as with arithmetic operations. The rule as to which expression must be chosen is built into the system: If x = B, then the Projection operation is not possible and so one defaults to Union. If x = T v C then Projection can proceed.

Negation of the result of either of the above operations can be accomplished by means of the transition laws between N and K already described. The only undesirable side-effect of this is the requirement to resolve ambiguity by choice when proceeding from N to K but as this is effectively forced by the structure of the

system (thus providing the law in the first place), it was not considered to be sufficient reason not to adopt this approach.

3.2.8 Reasons for abandoning a symbolic approach

The two obvious approaches to expanding GEL were to work on GEL(Q) which would have negative and positive initial vectors and GEL(|R|) which would be an expansion of GEL(|Q|) by finer discretisation. It was hoped that one or both of these approaches would show a reduction in ambiguity, in particular such that a delineation between the Union and Union over Atropy combinators would emerge. From the point of view of applicability to physical problems, it may also have been worth re-expressing the GEL concept to $G_{3,1}$, the geometric algebra over three geometric dimensions. This would have resulted in multiple levels of ectropy which may have provided the basis for a hierarchy of GEL systems in the same way that Haskell *et al.* were able to generate a hierarchy for biology, with one periodic coordinate system becoming the foundation of the next.

The decision was made not to pursue this hybrid numeric/symbolic approach for a number of reasons: Firstly, the amount of work to expand the system to include a greater resolution of magnitudes is beyond the scope of a project of this nature but, more importantly, the question as to whether or not it would be worth developing the

approach further is not definitely answered and would itself require a detailed investigation into the functional completeness and, consequently, the existence of an interpolation theorem for the system. The problems highlighted with implementing Boolean operations in GEL(|Q|) certainly do not bode well from this point of view and so the required time cannot be justified within the timescale of this project.

In order for GEL(|Q|) to be used in application to the problem addressed in this thesis, it is immediately necessary to expand it into three-dimensional space. This would require three-dimensional analogues of the qualitative value system and of the different operators that have been defined (projection, union, etc.); it would also most likely be necessary to define new operators for transformations between some of the new three-dimensional qualitative values. The resultant system would necessarily be geometrically more complex than the two-dimensional version discussed here (i.e. adding one spatial dimension would result in a many new qualitative values and operators). It would also need to be studied and analysed in the same way that GEL(|Q|) has been: verification of correctness of equivalences between the different domains on which the system is built, verification that existing laws still hold and/or identification of new laws, etc.

To determine if the additional work described above is worthwhile, it is important to analyse GEL(|Q|) from the point of view of internal completeness: If it does not possess the property of Functional Completeness (Post, 1941) then it is

likely that many equations will not be expressible in GEL(|Q|) since the system possesses no set of operators which can express all possible truth-tables. Unfortunately, it can be seen immediately from figures 3.5 and 3.6 that this is so; if it were not the case, there would be, on each figure, a line from each marked position on each axis to every other marked position on each axis. Since the system lacks functional completeness then it cannot possess an Interpolation Theorem (Hodges, 2005) meaning that there are derivations between equations expressed in GEL(|Q|) that will not be possible. The absence of these properties would require a very careful pre-emptive investigation of both GEL(|Q|) and its three-dimensional equivalent in order to ensure that the process of solving the EPI equation, once re-expressed in the system, would not be inhibited. Since the heuristic direction such problem-solving might take cannot be determined in advance, the decision to proceed with this symbolic approach would carry a very high risk, potentially exhausting a great deal of time only to produce an insurmountable structural obstacle. The decision was therefore made to look for an alternative approach.

Chapter Four

Constraint-logic programming: an alternative approach to the Kalman filter

4.0 Constraint-logic programming: an alternative approach to the Kalman filter

The purely symbolic approach detailed in the previous section is untenable due to the amount of depth to which it must be investigated. This parallels the standard approach to problem-solving of most humans. In order to imbue a computer with the ability to solve the EPI problem, a form of expression must be chosen that is both sufficiently abstract to allow automatic manipulation according to a clearly defined set of rules (i.e. requiring no interpretation or creativity) while retaining sufficient structure of the phenomenon being modelled to still make the resultant solution useful. Becker's (1976) work on dimensionless numbers turns out to be appropriate for this task.

It was originally intended to utilise Becker's (1976) work in order to automate the EPI process in a way that was both numerical and symbolic in nature (the hybridisation arising from the fact that the variables in an eigenratio represent magnitudes but are only worked with in terms of their abstract-meaning to the phenomenon in question). Since the goal in configurational-analysis is to acquire a configuration (a collection of eigenratios) for the phenomenon, a plan was constructed and partially implemented whereby a multi-agent system, with each agent implemented in the constraint-logic-programming paradigm, would 'argue out' the correct configuration for the expression of the EPI-equation for the turbulent

sound produced by blood flowing around an occlusion in the carotid artery. It turned out that this system did not need to be fully implemented since merely expressing the problem in a form that it could work with produced a single eigenratio configuration that provided the solution. Since the crux of the problem is the relationship between a macroscopic phenomenon of underlying microscopic activity (sound waves produced by the interaction of the molecules that compose human blood) and the error present in measurements of that phenomenon, the eigenratio is, necessarily, that composed of those two factors. The error-part of that eigenratio can easily be extracted from recordings of sound and a well known way of modelling macroscopic behaviour extrapolated from an underlying microscopic model, especially in the area of fluid-dynamics, is the cellular-automaton thus the solution of the EPI-equation is a cellular-automaton that is 'driven' by the error present in real-world data.

Having identified the correct representation of the problem in abstract terms, it is then possible to proceed with the development of a hybrid system, the first step being to find a cellular-automaton which is an appropriate model of the domain of said problem and whose accuracy can be varied automatically during the system's operation.

As a result of the multi-agent system already referred to, an abstract solution of the problem of imaging from one-dimensional acoustic data based around the Greenberg-Hastings cellular automaton (Fig. 7.1) can be acquired. This automaton

was originally developed to model oscillating chemical reactions but is appropriate to this project due to the obvious relation between this behaviour and that of sound-waves.

Figure 4.1: Evolution of Greenberg-Hastings rule.

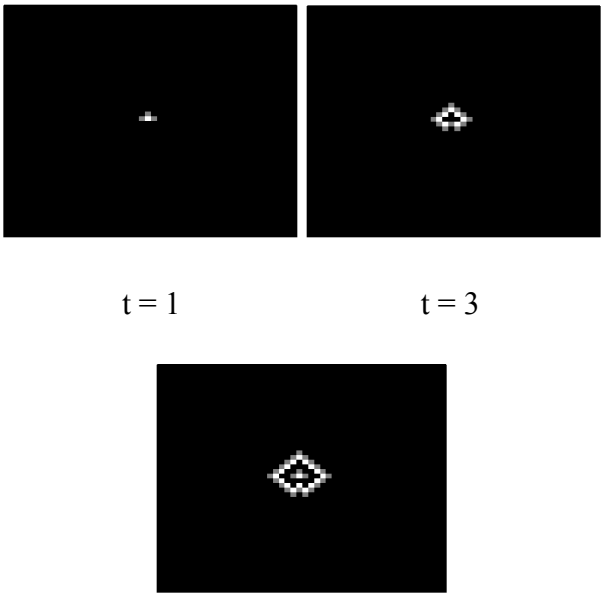

The question that arises once an appropriate cellular automaton model has been identified is then how to provide the algorithm with input in such a way that that input will control the accuracy of the simulation rather than serving as, for instance, the pattern to which the rules are applied. Complex and varying data make it unlikely that any such encoding could be developed that would work 100% of the time: testing the encoding method for every possible fluctuation in the input would take an unacceptably large amount of time. The alternative can be implemented by applying the work of Bagnoli (2008) which provides a method for the computation of

Maclaurin power series for totalistic cellular automata of which the Greenberg-Hastings rule is one. Using the definition of the boolean derivative (Vichniac, 1990) the *Ring Sum Expansion* (RSE) of the totalistic Greenberg-Hastings rule is produced. Its derivatives can then be computed and from this, a Maclaurin power series is formed. In practice, this is only done for part of the Diffusion function. The derivation proceeds as follows with σ representing the central cell of a given von Neumann neighbourhood and the σi representing the north, west, east and south cells relative to that cell:

The Greenberg-Hastings rule is given in terms of a reaction function R and a diffusion function D:

$$R(\sigma) = \{2 \textit{ if } \sigma = 1, \qquad \textbf{(4.1)}$$

$$\{0 \textit{ else}$$

$$D(\sigma_0, \sigma_1, \sigma_2, \sigma_3, \sigma_4) = \{1 \textit{ if } (\sigma_1 = 1 \textit{ or } \sigma_2 = 1 \textit{ or } \sigma_3 = 1 \textit{ or } \sigma_4 = 1) \textbf{ (4.2)}$$

$$\textit{and } \sigma_0 = 0$$

$$\{ 0 \text{ else.}$$

The complete rule can thus be expressed as R + D **(4.3)**

Conversion of partial diffusion rule (f) into RSE form:

$$f(\sigma_1, \sigma_2, \sigma_3, \sigma_4) = 1 \text{ if (one or more of } \sigma_1 \text{ through } \sigma_4 = 1) = f(T^{(4)}) \quad \textbf{(4.4)}$$

$f(T^{(4)}) = \sum_{k=1}^{4} r_k \wedge \chi_k$ where the χ_k are the *totalistic characteristic polynomials*:

(4.5)

$$\chi_1^{(4)} = \zeta_1 \oplus \zeta_3 \quad \textbf{(4.6)}$$

$$\chi_2^{(4)} = \zeta_2 \oplus \zeta_3 \quad \textbf{(4.7)}$$

$$\chi_3^{(4)} = \zeta_3 \quad \textbf{(4.8)}$$

$$\chi_4^{(4)} = \zeta_4 \quad \textbf{(4.9)}$$

and the ζ_i are homogeneous polynomials of degree i in the variables σ_1 through σ_4. The value of r_k is 1 if the rule f is 1 for k of the sites σ_1 through $\sigma_4 = 1$. The resultant ring sum expansion for f is:

$$\chi_1^{(4)} \oplus \chi_2^{(4)} \oplus \chi_3^{(4)} \oplus \chi_4^{(4)} \quad \textbf{(4.10)}$$

The final expression is $f(T^{(4)}) = \zeta_1 \oplus \zeta_2 \oplus \zeta_3 \oplus \zeta_4$ **(4.11)**

This expands to:

$$\sigma_1 \oplus \sigma_2 \oplus \sigma_3 \oplus \sigma_4 \oplus \sigma_1 \wedge \sigma_2$$

$$\oplus \sigma_1 \wedge \sigma_3 \oplus \sigma_1 \wedge \sigma_4 \oplus \sigma_2 \wedge \sigma_3$$

$$\oplus \sigma_2 \wedge \sigma_4 \oplus \sigma_3 \wedge \sigma_4$$

$$\oplus \sigma_1 \wedge \sigma_2 \wedge \sigma_3 \oplus \sigma_1 \wedge \sigma_2 \wedge \sigma_4$$

$$\oplus \sigma_1 \wedge \sigma_3 \wedge \sigma_4 \oplus \sigma_2 \wedge \sigma_3 \wedge \sigma_4 \oplus \sigma_1 \wedge \sigma_2 \wedge \sigma_3 \wedge \sigma_4$$

(4.12)

Using the definition of Boolean derivative, the partial derivatives of f are computed:

$$\frac{\partial f(T^{(4)})}{\partial \sigma_1} = 1 \oplus \sigma_2 \oplus \sigma_3 \oplus \sigma_4 \oplus (\sigma_2 \wedge \sigma_3) \oplus (\sigma_2 \wedge \sigma_4) \oplus (\sigma_3 \wedge \sigma_4)$$

$$\frac{\partial f(T^{(4)})}{\partial \sigma_2} = \sigma_1 \oplus 1 \oplus \sigma_3 \oplus \sigma_4 \oplus (\sigma_1 \wedge \sigma_3) \oplus (\sigma_1 \wedge \sigma_4) \oplus (\sigma_3 \wedge \sigma_4)$$

$$\frac{\partial f(T^{(4)})}{\partial \sigma_3} = \sigma_1 \oplus \sigma_2 \oplus 1 \oplus \sigma_4 \oplus (\sigma_1 \wedge \sigma_2) \oplus (\sigma_1 \wedge \sigma_4) \oplus (\sigma_2 \wedge \sigma_4)$$

$$\frac{\partial^2 f(T^{(4)})}{\partial \sigma_1 \partial \sigma_2} = 1 \oplus \sigma_3 \oplus \sigma_4 \oplus (\sigma_3 \wedge \sigma_4)$$

$$\frac{\partial^2 f(T^{(4)})}{\partial \sigma_1 \partial \sigma_3} = 1 \oplus \sigma_2 \oplus \sigma_4 \oplus (\sigma_2 \wedge \sigma_4)$$

$$\frac{\partial^2 f(T^{(4)})}{\partial \sigma_1 \partial \sigma_4} = 1 \oplus \sigma_2 \oplus \sigma_3 \oplus (\sigma_2 \wedge \sigma_3)$$

$$\frac{\partial^2 f(T^{(4)})}{\partial\sigma_2\partial\sigma_3} = \sigma_1 \oplus 1 \oplus \sigma_4 \oplus (\sigma_1 \wedge \sigma_4)$$

$$\frac{\partial^2 f(T^{(4)})}{\partial\sigma_2\partial\sigma_4} = \sigma_1 \oplus 1 \oplus \sigma_3 \oplus (\sigma_1 \wedge \sigma_3)$$

$$\frac{\partial^2 f(T^{(4)})}{\partial\sigma_3\partial\sigma_4} = \sigma_1 \oplus \sigma_2 \oplus 1 \oplus (\sigma_1 \wedge \sigma_2)$$

$$\frac{\partial^3 f(T^{(4)})}{\partial\sigma_1\partial\sigma_2\partial\sigma_3} = 1 \oplus \sigma_4$$

$$\frac{\partial^3 f(T^{(4)})}{\partial\sigma_1\partial\sigma_2\partial\sigma_4} = 1 \oplus \sigma_3$$

$$\frac{\partial^3 f(T^{(4)})}{\partial\sigma_1\partial\sigma_3\partial\sigma_4} = 1 \oplus \sigma_2$$

$$\frac{\partial^2 f(T^{(4)})}{\partial\sigma_3\partial\sigma_4} = \sigma_1 \oplus \sigma_2 \oplus 1 \oplus (\sigma_1 \wedge \sigma_2)$$

$$\frac{\partial^3 f(T^{(4)})}{\partial\sigma_1\partial\sigma_2\partial\sigma_3} = 1 \oplus \sigma_4$$

$$\frac{\partial^3 f(T^{(4)})}{\partial\sigma_1\partial\sigma_2\partial\sigma_4} = 1 \oplus \sigma_3$$

$$\frac{\partial^3 f(T^{(4)})}{\partial\sigma_1\partial\sigma_3\partial\sigma_4} = 1 \oplus \sigma_2$$

$$\frac{\partial^3 f(T^{(4)})}{\partial\sigma_2\partial\sigma_3\partial\sigma_4} = 1 \oplus \sigma_1$$

$$\frac{\partial^4 f(T^{(4)})}{\partial\sigma_1\partial\sigma_2\partial\sigma_3\partial\sigma_4} = 1$$

(4.12 - 4.30)

This allows the derivation of a Maclaurin power series representation of f:

$$
\begin{aligned}
f_{t+1}(T^{(4)}) = f(0^{(4)}) \oplus \sigma_1 \wedge \left.\frac{\partial f}{\partial \sigma_1}\right|_{0^{(4)}} \oplus \sigma_2 \wedge \left.\frac{\partial f}{\partial \sigma_2}\right|_{0^{(4)}} \\
\oplus \sigma_3 \wedge \left.\frac{\partial f}{\partial \sigma_3}\right|_{0^{(4)}} \oplus \sigma_4 \wedge \left.\frac{\partial f}{\partial \sigma_4}\right|_{0^{(4)}} \oplus \\
\sigma_1 \wedge \sigma_2 \wedge \left.\frac{\partial^2 f}{\partial \sigma_1 \partial \sigma_2}\right|_{0^{(4)}} \oplus \sigma_1 \wedge \sigma_3 \wedge \left.\frac{\partial^2 f}{\partial \sigma_1 \partial \sigma_3}\right|_{0^{(4)}} \\
\oplus \sigma_1 \wedge \sigma_4 \wedge \left.\frac{\partial^2 f}{\partial \sigma_1 \partial \sigma_4}\right|_{0^{(4)}} \oplus \sigma_2 \wedge \sigma_3 \wedge \left.\frac{\partial^2 f}{\partial \sigma_2 \partial \sigma_3}\right|_{0^{(4)}} \\
\oplus \sigma_2 \wedge \sigma_4 \wedge \left.\frac{\partial^2 f}{\partial \sigma_2 \partial \sigma_4}\right|_{0^{(4)}} \oplus \sigma_3 \wedge \sigma_4 \wedge \left.\frac{\partial^2 f}{\partial \sigma_3 \partial \sigma_4}\right|_{0^{(4)}} \\
\oplus \sigma_1 \wedge \sigma_2 \wedge \sigma_3 \wedge \left.\frac{\partial^3 f}{\partial \sigma_1 \partial \sigma_2 \partial \sigma_3}\right|_{0^{(4)}} \\
\oplus \sigma_1 \wedge \sigma_2 \wedge \sigma_4 \wedge \left.\frac{\partial^3 f}{\partial \sigma_1 \partial \sigma_2 \partial \sigma_4}\right|_{0^{(4)}} \\
\oplus \sigma_1 \wedge \sigma_3 \wedge \sigma_4 \wedge \left.\frac{\partial^3 f}{\partial \sigma_1 \partial \sigma_2 \partial \sigma_4}\right|_{0^{(4)}} \\
\oplus \sigma_2 \wedge \sigma_3 \wedge \sigma_4 \wedge \left.\frac{\partial^3 f}{\partial \sigma_2 \partial \sigma_3 \partial \sigma_4}\right|_{0^{(4)}} \oplus \\
\sigma_1 \wedge \sigma_2 \wedge \sigma_3 \wedge \sigma_4 \wedge \left.\frac{\partial^4 f}{\partial \sigma_1 \partial \sigma_2 \partial \sigma_3 \partial \sigma_4}\right|_{0^{(4)}}
\end{aligned}
\qquad \textbf{(4.31)}
$$

Given that the partial derivatives in the above expression each evaluate to true given the false-neighbourhood ($0_{(4)}$: north, west, east and south sites all false) and f itself evaluates to false, we are left with the far simpler expression:

$$f_{t+1}(T^{(4)}) = \sigma_1 \oplus \sigma_2 \oplus \sigma_3 \oplus \sigma_4 \oplus \sigma_1 \wedge \sigma_2 \\ \oplus \sigma_1 \wedge \sigma_3 \oplus \sigma_1 \wedge \sigma_4 \oplus \sigma_2 \wedge \sigma_3 \oplus \sigma_2 \wedge \sigma_4 \\ \oplus \sigma_3 \wedge \sigma_4 \oplus \sigma_1 \wedge \sigma_2 \wedge \sigma_3 \oplus \sigma_1 \wedge \sigma_2 \wedge \sigma_4 \\ \oplus \sigma_1 \wedge \sigma_3 \wedge \sigma_4 \oplus \sigma_2 \wedge \sigma_3 \wedge \sigma_4 \\ \oplus \sigma_1 \wedge \sigma_2 \wedge \sigma_3 \wedge \sigma_4 \qquad \textbf{(4.32)}$$

This expression is identical to the RSE representation of f from the start of the derivation and so it is actually a proof that has been undertaken; it is nevertheless still important as, for a nonlinear model such as this, it is irresponsible to make assumptions regarding the properties of the rules.

By varying the degree of truncation of the power series representation based upon the amount of error present in the data, the Greenberg-Hastings model can be used to create a two-dimensional profile of the one-dimensional data exposing information that was previously obscured in the lower-dimensional representation. For ease of reference in the following text, we will refer to this algorithm as a *Driven Cellular Automaton* (DCA).

4.1 Practical considerations

In order to use the available data in a way consistent with the EPI approach, it is necessary to perform a quantisation so that different levels of noise present in the

data can be mapped to the number of terms to which the power series is truncated. The automated configurational analysis performed indicates that the signal to noise ratio (SNR) should be used for this purpose. A pair of second-order Butterworth filters, one low-pass and one high-pass are therefore used to extract, respectively, the signal and the noise. The power of each of these components is then computed and used to compute the SNR. Using parameters determined pragmatically, this computation is performed on windows of the signal 1/10th of the sample-rate in length. The cutoff point for the filters is determined from manual examination of the data's spectrogram.

The nonlinear nature of the algorithm means that attention must be paid to the number of iterations as a strong resultant pattern can be obliterated in a single cycle. The system is therefore limited to 25 iterations as this allows the corners of the classical Greenberg-Hastings pattern shown in Figure 1 to reach the boundaries of the cellular space. These boundaries are actually defined to be periodic which provides the possibility of a 'second-order' pass were the algorithm allowed to run for another 25 iterations but without fully analysing the 'first-order' patterns, it would be unwise to attempt to tackle the additional complexity that this would introduce.

With a limitation of 25 iterations, combined with a pragmatically determined window-size of 4410 samples (for a recording with a sample rate of 44.1kHz), we

can therefore analyse 2.5 seconds of sound. Given that the pitch-perception threshold for the frequencies involved in the kind of turbulence dealt with is at most approximately 100ms (Roads, 2004) and taking into account that it is possible for a human to make reasonable inferences about an artery merely from listening to it through a stethoscope, it is reasonable to expect that this length of recording will contain all of the information that any recording made by the same method would be able to provide.

A typical cutoff frequency is 4000 Hz but this choice is dependent upon the background noise present at the location in which a recording is taken and is identified from the recording's spectrograph.

For a given recording, the minimum and maximum SNRs are computed in advance and the range [SNR_{min}, SNR_{max}] is divided into 'bands' numbering the quantity of terms present in the Maclaurin expansion of the Greenberg-Hastings diffusion function (minus the conjunction with the central site as already discussed). This means that for the standard Greenberg-Hastings automaton, there are 15 possible bands. While this might seem on first inspection like a very low granularity, it will be shown (see chapters 8 and 9) that the nonlinear nature of the cellular automaton makes the technique sufficiently sensitive even so.

The resultant algorithm adapts a non-linear model (the Greenberg-Hastings

cellular automaton) in such a way that it is driven by fluctuations in the SNR of the input data (the sound caused by turbulence in the simulated occluded carotid artery). The nonlinear nature of the cellular automaton means that a slight change to its algorithm results in a large change in the generated pattern, even within a single iteration of the system. This change is achieved by truncating the part of the diffusion function that has been proven equivalent to a Maclaurin power series to a number of terms determined by the SNR. Since each iteration generates its pattern based on the preceding one, the system therefore produces a cumulative effect resulting in distinct final patterns based on both the magnitude and order of occurrence of SNR fluctuations.

Chapter Five

Results and Discussion

5. Results and Discussion

5.1 Quantitative results

The system was developed to create rich profiles of acoustic data. The requirement is that carotid artery plaques can be imaged but, as a necessary part of such a geometric representation is magnitude, the initial tests performed were focused purely on this as a failure in this area would mean that the approach as a whole was unsuccessful in its current form. Physical simulations were created of a non-occluded artery along with arteries involving approximately 30%, 60%, 90% occlusions. The resultant images after 25 iterations were as follows:

Figure 5.1a: Waveform, spectrum and final output of system after 25 iterations on 0% and 30% occlusion**.**

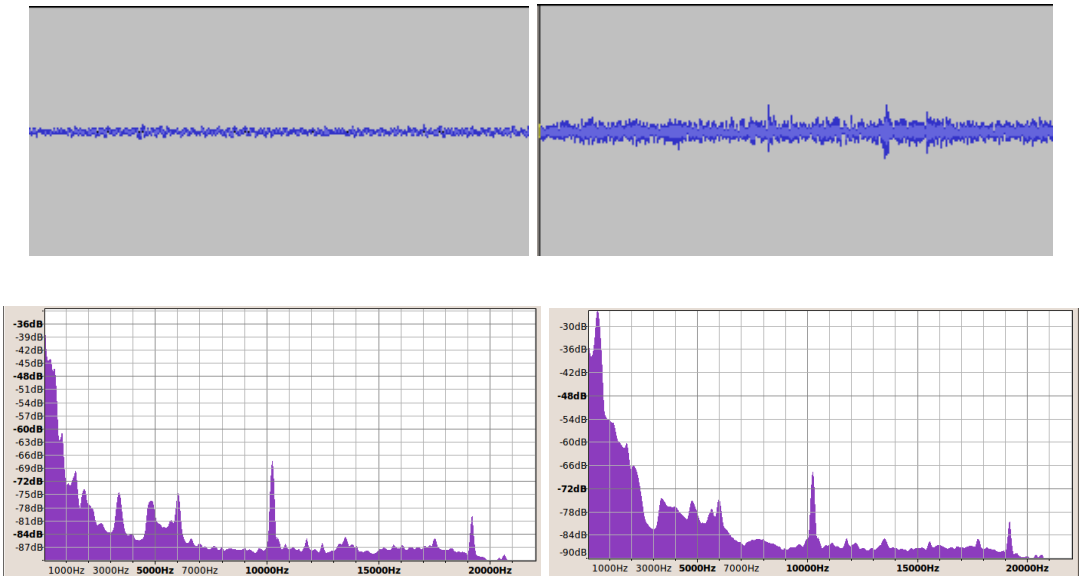

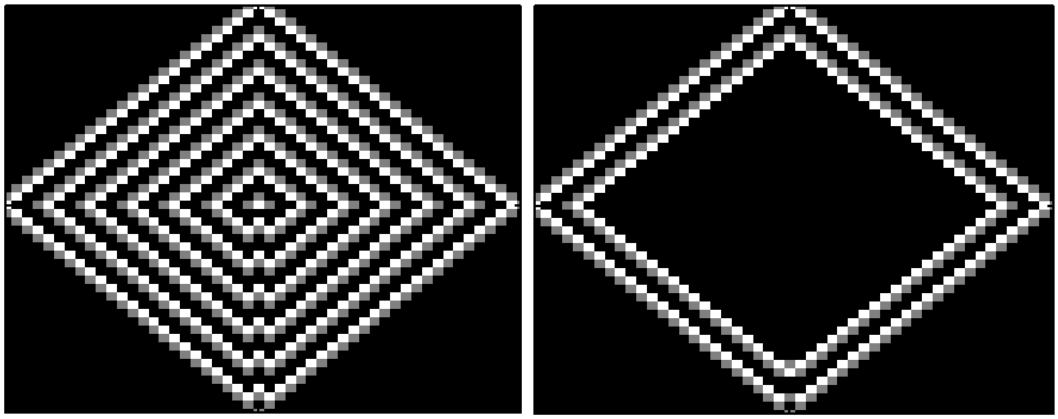

0% 30%

Figure 5.1b: Waveform, spectrum and final output of system after 25 iterations on 60% and 90% occlusion**.**

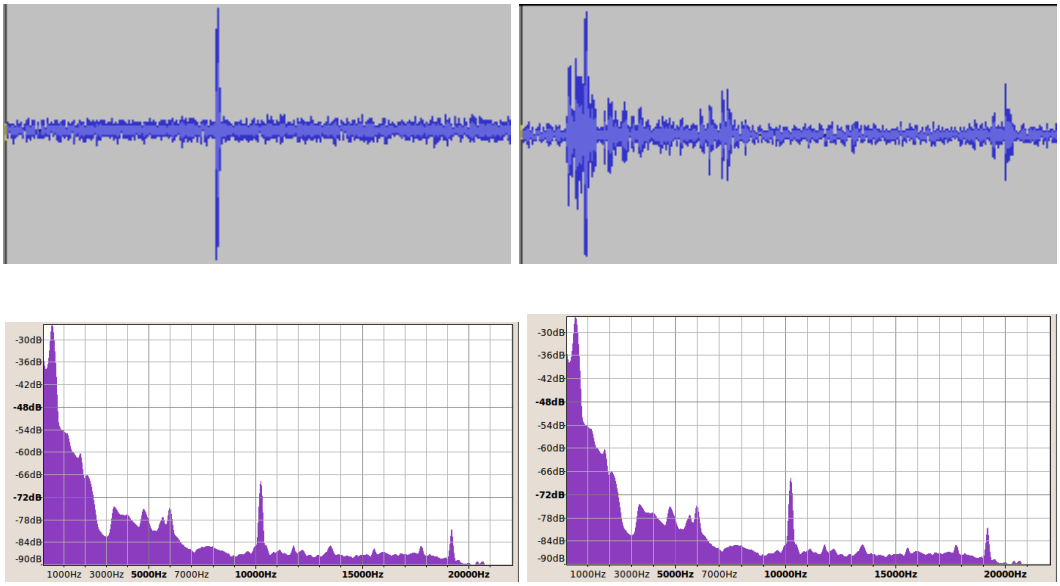

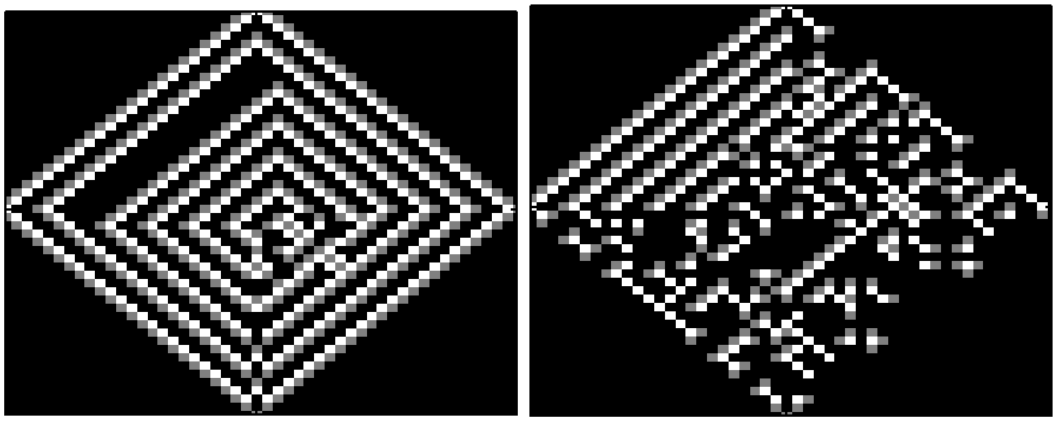

60% 90%

The images in Figures 5.1a and 5.1b are typical of the output of the system although there are variances between runs on different recordings of the same occlusion. At this stage however, it was felt that a potential for the system to produce distinct signatures for different levels of occlusion had been demonstrated, making the approach worthy of further development. The interpretation of the images in more detail (i.e. to extract more detailed information about a plaque) was deferred at this stage due to the lack of interest in geometric information. It seems reasonable to say that the Greenberg-Hastings representation conveys the differences between the different levels of occlusion more strongly than the spectrum plot but perhaps only equalling the communicative capacities of the waveforms themselves. The extraction of geometric/topological information was expected to be the main advantage of processing sound in this way due to the ‘smearing’ discussed above.

5.1.1 Notes of caution

The nonlinear nature of the algorithm makes the system extremely sensitive to fluctuations in the data. It is this sensitivity that allows the system to generate distinctive patterns for the different levels of occlusion but this ability comes at a cost. Cellular automata are renowned for nonlinear behaviour and in this case, there are effectively 15 different rules which can be applied at any given time instant resulting in extremely unpredictable behaviour in some cases. Instances were observed whereby a pattern evolved in a reasonably continuous way only to completely change in a single iteration. This suggested that merely considering the final pattern of a series of iterations may not be sufficient to extract the maximum amount of information available from the model and that we should therefore analyse the various intermediate patterns that appear and disappear. Ultimately, this has seemed to be unnecessary but the point is still recorded here in case it is of relevance to further work beyond the scope of this project.

5.2 Topological results

Having determined that the system produces distinct images for sounds-recordings taken from arteries afflicted by different levels of occlusion, the next stage was to test its ability to respond to differences in plaque-topology.

The images produced from the system described in the previous chapter were informative for the plaque-topologies tested but were not considered distinct enough to allow quick and easy analysis by a user who is not in possession of detailed knowledge of the underlying algorithms. For this reason, the two-dimensional images were treated as terrain-maps for three-dimensional rendering with the third-dimension being provided by overlaying the amplitudes values of the original recording on this map and using them to provide the height of the peaks. This approach increases the amount of variation between different output images.

Artificial plaques were constructed from polymorph with the following properties:

Figure 5.2: p1 - A plaque consisting of an approximately hemispherical mound. (Short-name: Blob-mound).

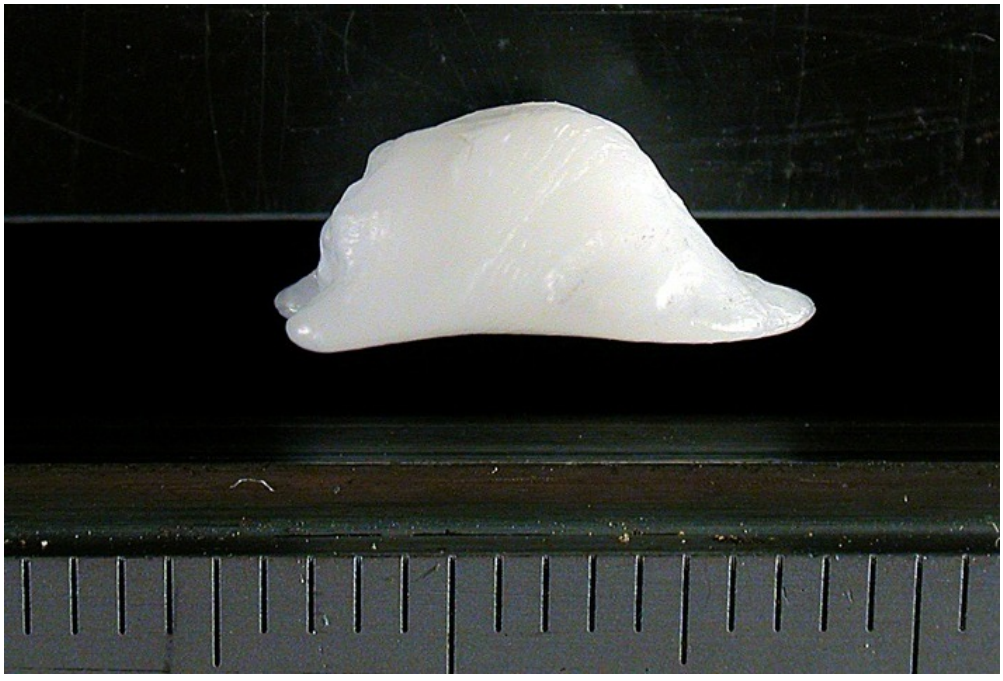

(scale in mm)

Figure 5.3: p2 - A square version of the hemispherical mound. (Short-name: Blob-square).

(scale in mm)

Figure 5.4: p3 - A small thin ridge shape. (Short-name: Thin-ridge small).

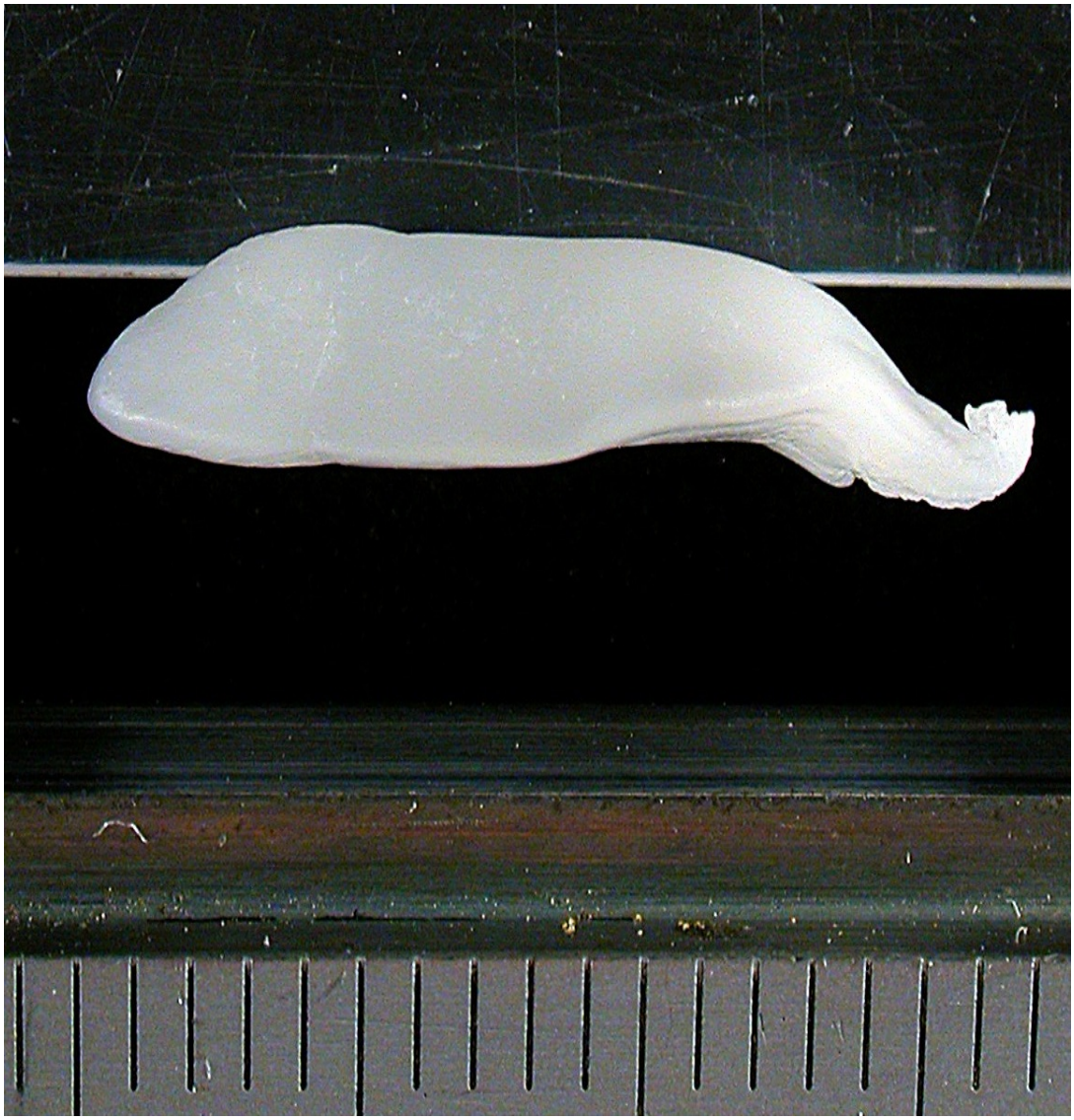

(scale in mm)

Figure 5.5: p4 - A more bulbous ridge shape. (Short-name: Fat-ridge small).

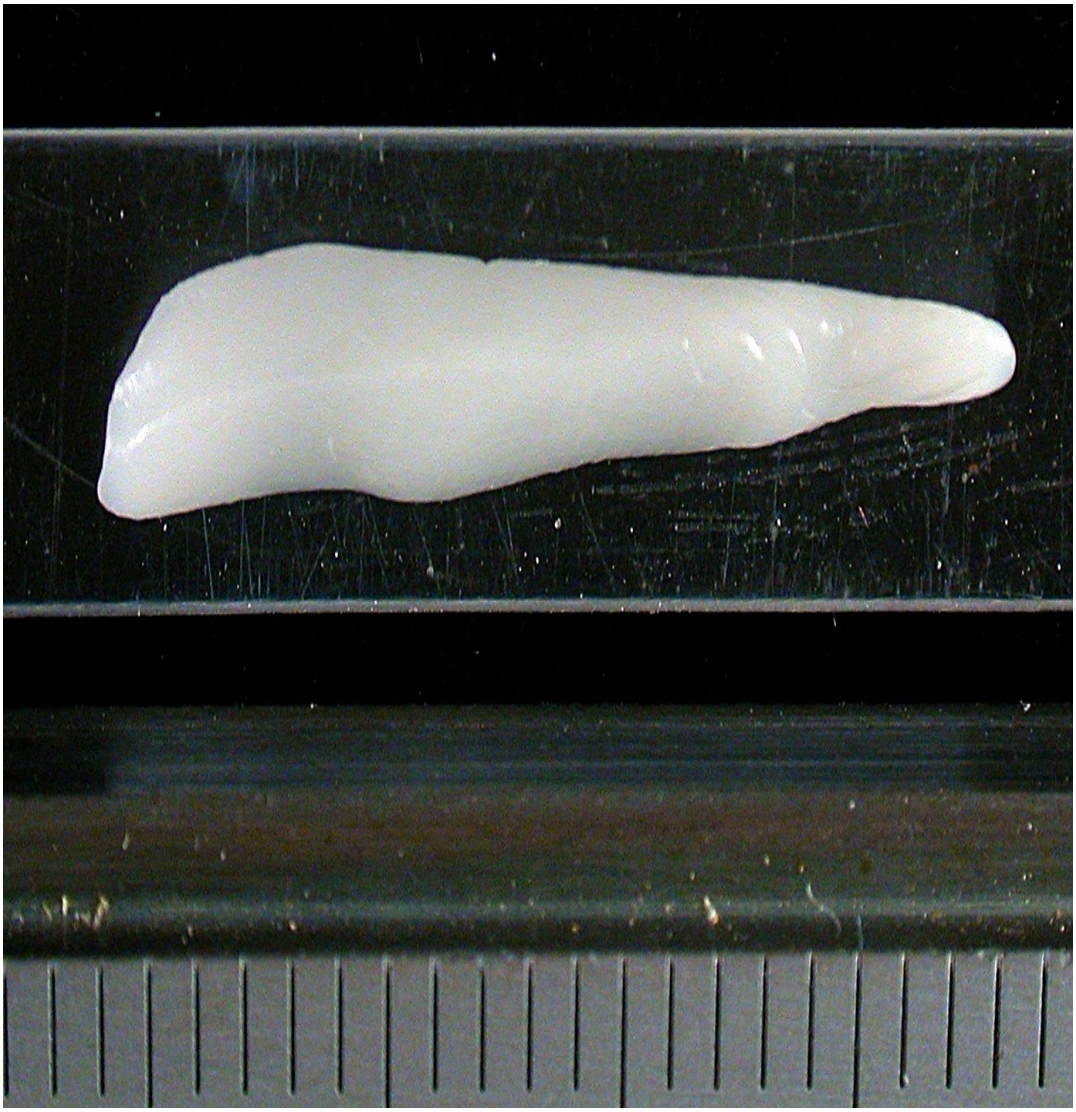

(scale in mm)

Figure 5.6: p5 - A larger version of fat-ridge small.

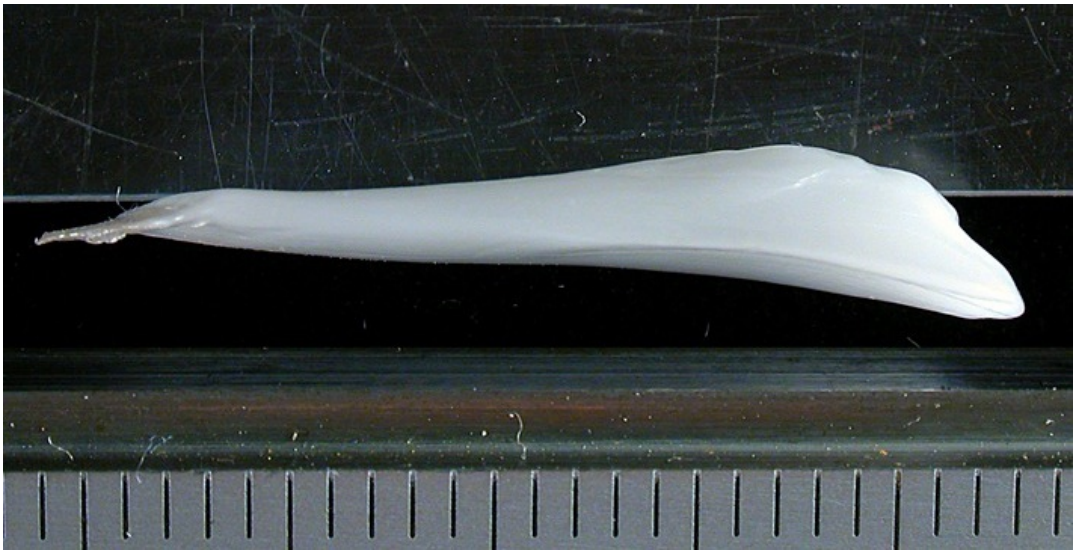

(scale in mm)

Figure 5.7: p6 - A small plaque with stalagmite-like protrusions (Short-name: Small-pokey).

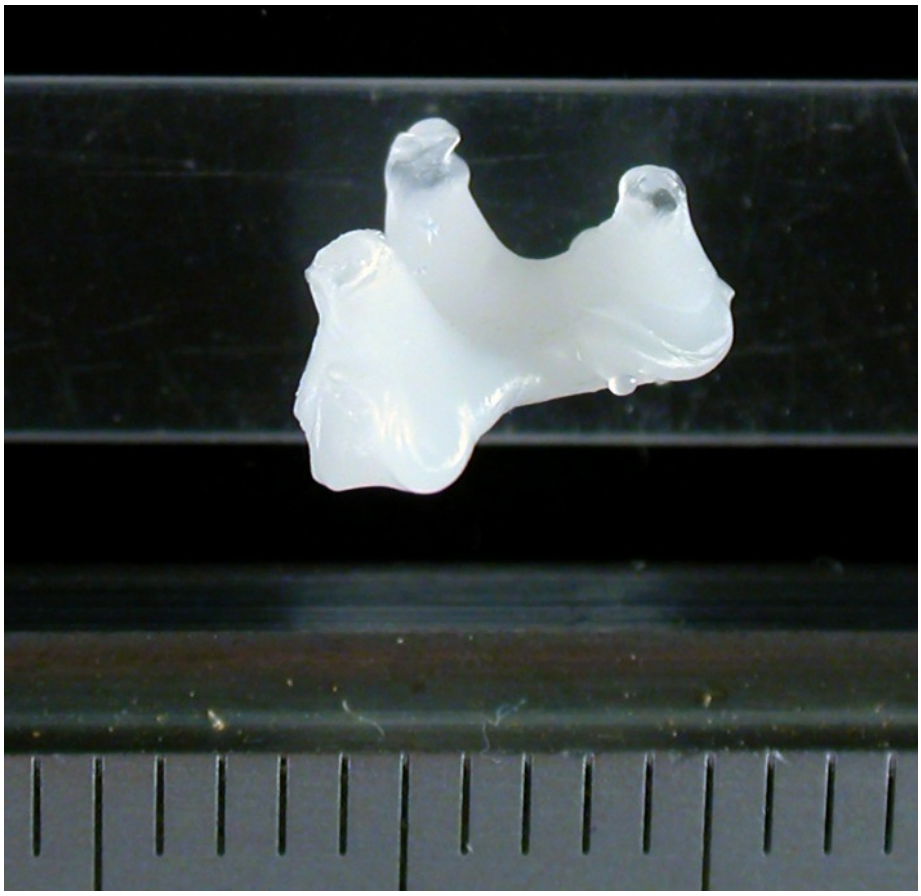

(scale in mm)

Figure 5.8: p7 - A larger version of small-pokey.

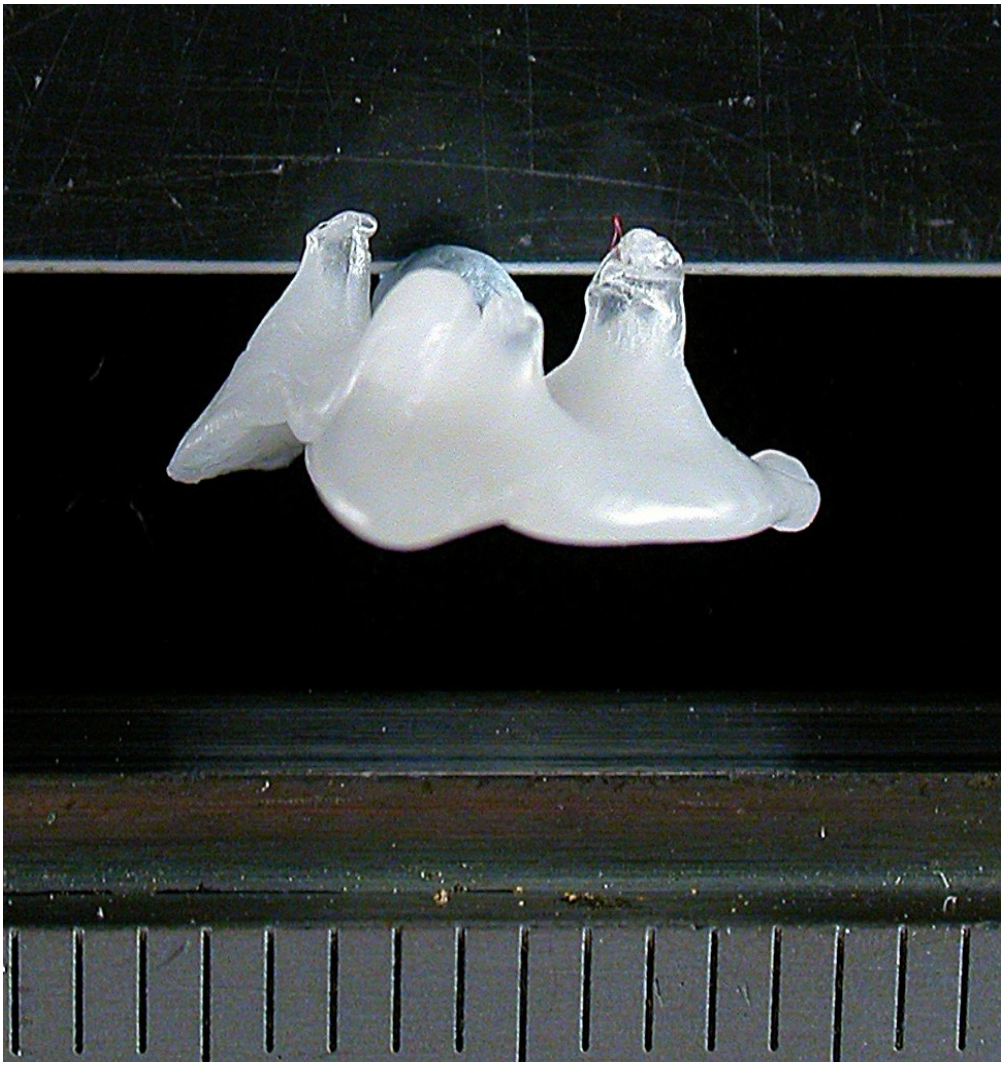

(scale in mm)

5.2.1 Procedure

Recordings were taken with water-flowing at the same speed as for the quantitative tests in the previous chapter. Each recording was taken over 10 seconds to allow the data to be broken up into 4 repeat runs of 2.5 seconds each.

The rendered images for the different plaque-topologies look as follows:

Figure 5.9a: System output for plaque p1 (Blob-mound).

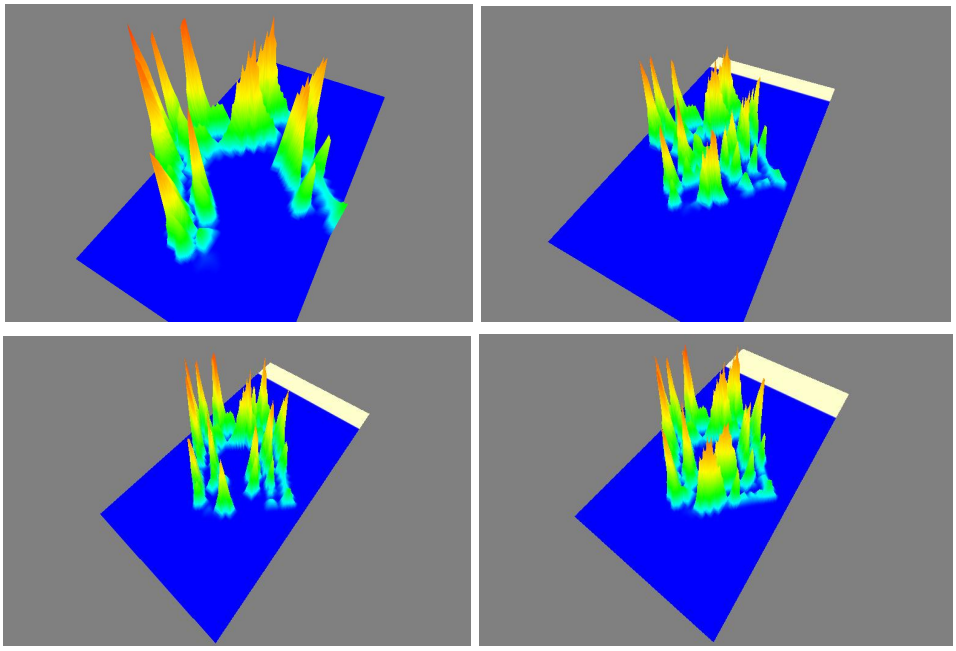

Figure 5.9b: System output for plaque p2 (Blob-square).

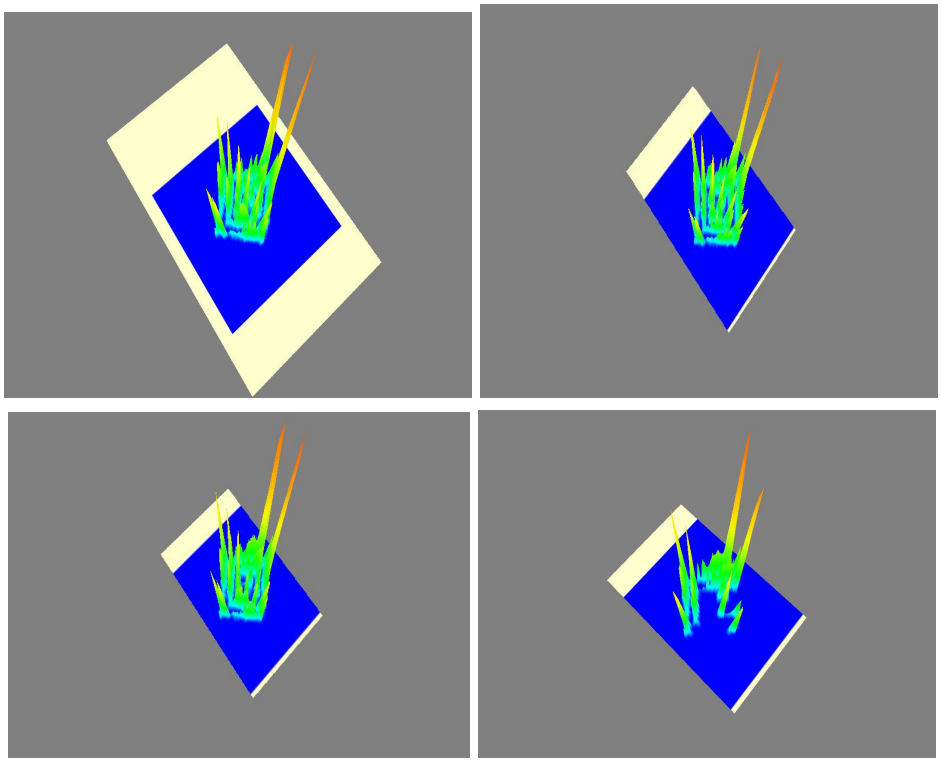

Figure 5.9c: System output for plaque p3 (Thin-ridge small).

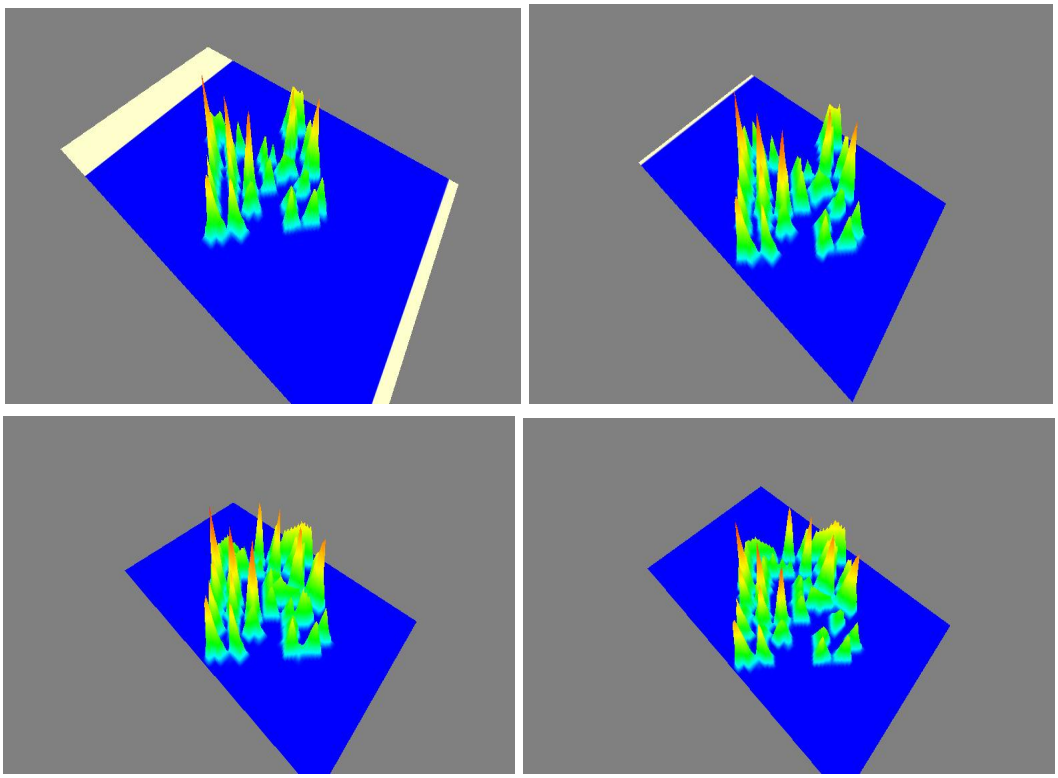

Figure 5.9d: System output for plaque p4 (Fat-ridge small).

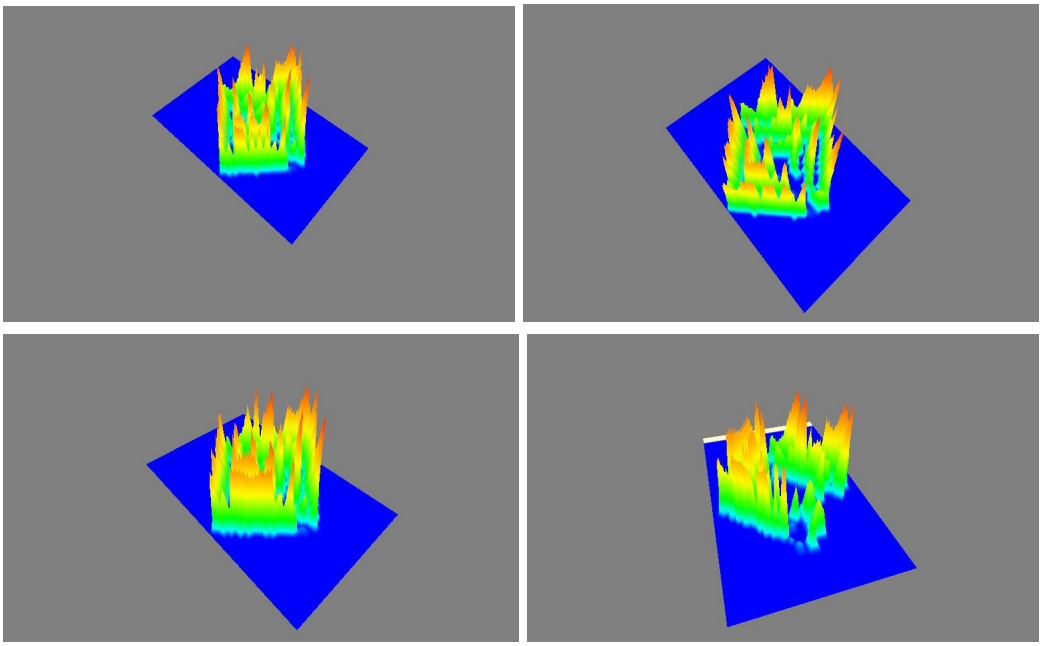

Figure 5.9e: System output for plaque p5 (Fat-ridge large).

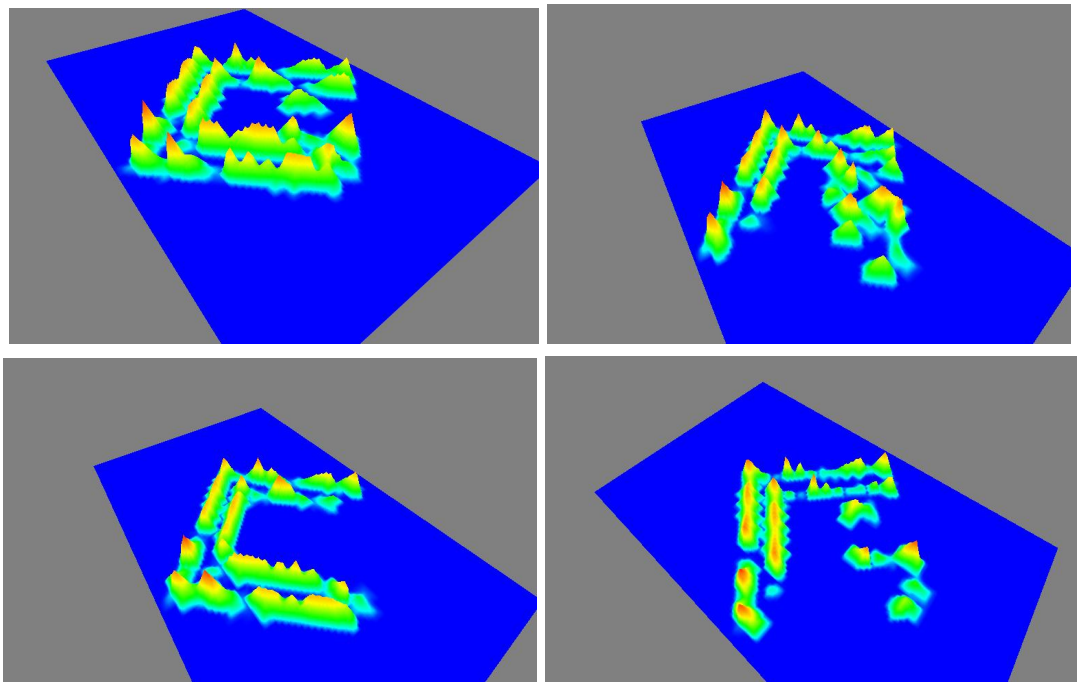

Figure 5.9f: System output for plaque p6 (Small-pokey).

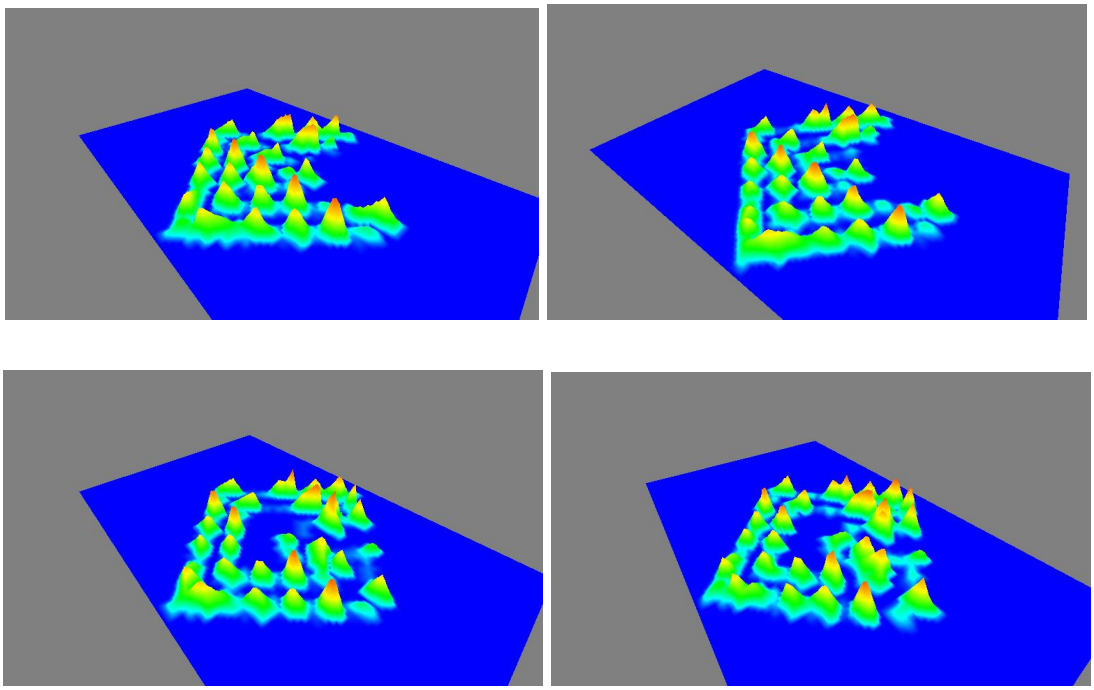

Figure 5.9g: System output for plaque p7 (Large-pokey).

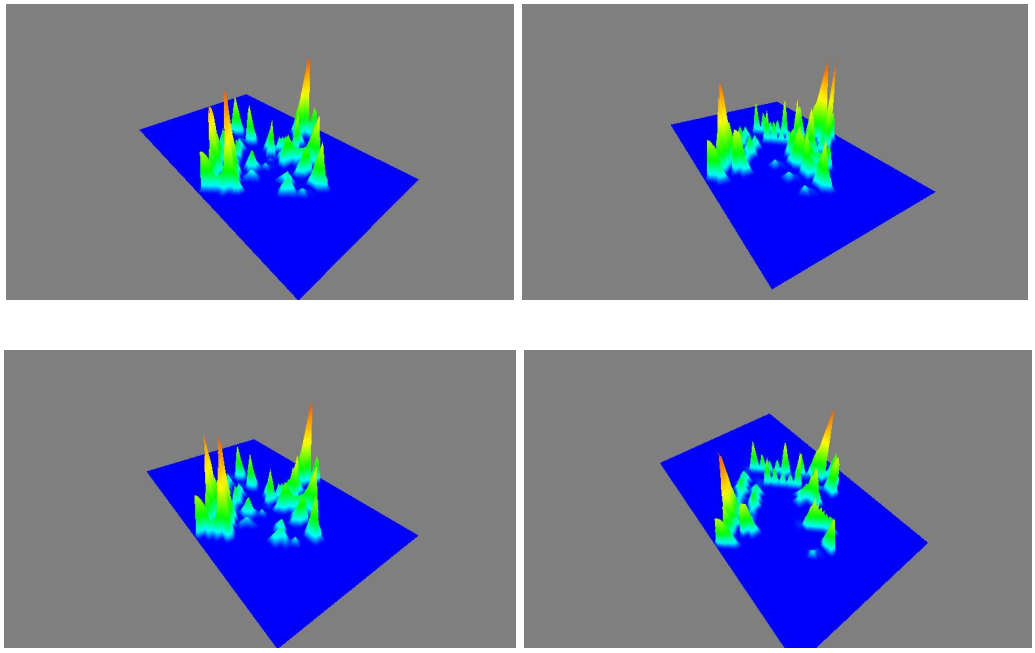

5.2.2 Analysis

5.2.2.1 Axiomatic basis

It is helpful to begin by defining certain criteria that one would reasonably expect from the images produced by the system. These criteria are considered to be axiomatic in that they are self-evident, requiring only simple logical reasoning about the apparatus and the phenomenon under investigation in order to satisfy us as to their appropriateness.

1. Contrast: No two plaque topologies should produce the same image

topologies.

2. Signature: Minor variations are acceptable between runs but there should be an indisputable

common 'essence' shared by all of the images for a given plaque-topology.

3. Scalability: The same topology in different sizes should produce similar images, ideally with only a variance in size in the image-topology.

As to the first of these criteria, it is clear that the system responds differently and distinctly for each of the topologies tested. The most significant point to draw from a comparison in this context is that the crucial aspects that result in different signatures appear to be 'base-pattern' (the tendency for certain areas of the grid to always contain peaks for a given plaque-topology) and 'inter-peak ratio' (the distribution of high and low peaks is close to constant for a given plaque-topology).

Regarding the criterion of signature, it would seem to be self-evident that for a given plaque-topology, the four runs always share enough features to allow an image from that group to be easily matched against another from the same group.

The most useful plaque-topologies for an analysis of scalability are: Fat-ridge small vs. Fat-ridge large and Small-pokey vs. Large-pokey. These image-topologies, while not only affected by scale, do seem to indicate that the basic signature of the form is preserved between small and large versions. It is interesting to note that for

the fat-ridge plaques, an increase in size corresponds to a *decrease* in peak-height but for the 'pokey' topology, the opposite is almost true. Intuitively, it would seem reasonable that the ridge shape, being far more uniform than the a plaque consisting of several different protrusions, would result in less variance in its resultant image-topology.

It can be seen that the images displayed are not actual pictures of the simulated plaques. This is not however important within the context of medical semiotics where, even in cases where a medical-imaging system produces signs intended to represent their objects in respect of their actual existence (i.e. a photograph of your friend is exactly that; it doesn't require interpretation to discern what it is), diagnostic analysis is still based upon the recognition and interpretation of abstractions (for instance, in the case of the Roentgen Semiotics of x-ray images sharp changes in contrast and unusual distribution of light and dark areas are of far more use than treating the image as a photograph (Cantor, 2000)). The important part of the semiotic triangle is therefore the interpretant rather than the sign. As with the initial axioms, the formation of interpretants must be consistent but it is also reasonable to require the user to be trained for what to look for (as is the case with virtually every existing medical imaging system). It is the result of the diagnosis that is important not how we get there and in the case of the system described here it is actually the most abstract part of the semiotic triangle that is the more practical. We can demonstrate this relatively easily by consideration of Peirce's process of infinite

semiosis applied to both indexical and symbolic images. To briefly recap, an indexical sign is in some way a *physical consequence* of its object whereas a symbolic sign is connected to its object by either resemblance of an abstraction or by convention (as in the case of a WC sign).

X-rays and MRI images contain only indexical signs (‘contain’ is very significant here since an image from either system is not really a sign in itself). When a trained expert views such an image, they form interpretants triggered by the presence or absence of certain more abstract indexical signs like lines, curves and shadows (as in those dealt with by Roentgen Semiotics). The first interpretant (let's say, the presence of a shadow where one would not normally be expected) is a sign in itself and therefore gives rise to another interpretant which may give rise to another and so on up to the point where the certainty of the interpretation is considered sufficient for it to become a diagnosis (such as the presence of tuberculosis). This diagnosis is a new sign but is symbolic in nature - it is a statement of the existence of a phenomena but it does not represent it in terms of the nature of its existence. The object in question (in this case the actual physical matter present in the patient's lung) will never be fully signified by either the sign or by the resultant interpretants.

Now consider the semiotic process involved in the interpretation of a driven cellular-automaton image. Whilst physically caused by the phenomenon in question,

the set of all possible images that the system can produce is not in an isomorphic relationship with the set of all possible plaques and so we cannot say that the signs in such an image are indexical. They are symbolic but from there the process of semiosis is exactly the same as it is in our X-ray example. A trained user will recognise certain features of the image and this recognition will necessarily involve the creation of an interpretant sign which will possibly lead to the creation of more interpretants until a diagnosis is decided upon. This diagnosis is now symbolic in nature, just as it is in the X-ray.

To demonstrate that DCA image analysis is in fact virtually identical to X-ray or MRI analysis, we now only need to point out that neither an indexical or symbolic sign is the object in Peirce's triadic model and it is suddenly not so unreasonable to refer to the DCA as a medical imaging system in the context of this work.

Having passed examination by the initial axioms then, it is necessary to identify a concrete (i.e. dealing with specific signs within the domain being discussed as opposed to general principles) semiotics of the output of the system. The process of placing the topological results along with the quantitative results of the previous chapter within a framework of interpretation derived from existing medical imaging practice will validate this study within its domain and this forms the majority of the remaining work.

5.2.2.2 A semiotic formalisation of DCA image analysis

It is considered a suitably rigorous test of the Driven Cellular Automaton's ability to produce images that are useful in a medical-diagnosis context that it should be possible to construct an analogue of the fundamental principles of Roentgen Semiotics; this would mean that it is possible to study DCA image-analysis in the same way that it is possible to study the analysis of X-rays and this must inexorably mean that X-rays are useful to medics in the same way.

We proceed by defining analogues to the concepts used in Cantor's semiotics analysis of X-ray interpretation of which the fundamental sign is that of the 'radiographic boundary', defined as "the interface between contiguous regions of a radiograph that are distinguished by visual contrast". This idea is subsequently broken down into the different kinds of visual contrast possible in an X-ray image and, within that breakdown, the more subtle signs of 'loss', 'gain' and 'exchange' of visual-contrast signs. An example might be that, for a broken bone, the X-ray *gains* a *line-separation*. Both of the italicized terms refer to signs, the *line-separation* being only visual (we can see that it is there simply by looking) while the *gain* is rooted in the interpretant (i.e. whether or not we consider the line-separation to mean anything is dependent upon our knowledge that it would not normally be there).

It is clear that in order to analyse DCA images in a similar way, we must first

define the analogue of a radiographic-boundary. In our output images which are three-dimensional in nature, we do this by considering the difference between the image produced for blood-flow in an unoccluded artery and that for an artery occluded in some way (that way being irrelevant at this high level of analysis). Since the image for an unoccluded artery is simple a plane (with, perhaps a few minor artefacts), we can consider the first level of semiotic distinction to be any projection perpendicular to that plane. We will name this distinction the *topological-boundary* and, at the highest level of interpretation, we can state that the *gain* of a *topological-boundary* from a flat-plane always signifies illness (most likely but not necessarily an occlusion of the carotid-artery) and that the loss of ALL topological-boundaries signifies a loss of illness (i.e. recovery) but note that this sign is more focussed in the interpretant than the representamen since it is dependent upon knowledge of the patient's case-history. From any sign which is not the flat-plane, loss or gain of topological boundaries is only useful in comparison to previous images and so while the reason for all of the signs of this kind with the exception of crude presence or absence of a topological-boundary being rooted in the interpretant is not entirely the same as it is for X-rays (general medical knowledge is necessary to interpret a new sign as described in the example above and knowledge of the patient's case-history is necessary otherwise), it is actually still a subset of that reason (case-history is necessary to interpret gains and losses from non-flat-plane images but the interpretation of the first DCA image every made for a patient does NOT require general-medical knowledge since, if a topological-boundary is present,

even a layman could immediately make a correct diagnosis (that there is a problem) albeit a crude one.

Beyond this first level of interpretation, gain and loss are useful only in a secondary respect which is to say that the gain or loss is only useful if we know what was gained or lost *from* as well as the meaning of the *current* image. At this point, the three-dimensional nature of DCA images comes to the forefront and we find that we can define the following categories if we remember that words like 'equal' and 'enclose' are not strict mathematical terms but terms that could be used by a human inspecting the DCA images without instrumentation (a ruler for instance) for this support of informal, 'at a glance' analysis is a requirement if the system is to be useful at the same level of diagnosis as X-rays:

Table 5.1: Semiotic categories for DCA image analysis

Altitude	The height of the peaks present in an image which has gained a topological boundary. This sign is quantitative in nature.
Altitudinal homogeneity	Whether or not the peaks in an image are of approximately the same height or not. This is sign is possessive in nature - an image either has it or doesn't as can be seen from the example images; there is no situation where exact altitudinal homogeneity has a different meaning to slightly less altitudinal homogeneity.
Phase regularity	Whether or not the peaks appear at equally-spaced intervals.
Planar completeness	Knowing what we do about the normal shape of the patterns

	produced by a Greenberg-Hastings cellular automaton, is there a peak (of any altitude) for each cell? At the time of writing, this sign would appear to be possessive in nature, at least from the point of view of what we can diagnose from it.
Enclosure	Does one area of the image enclose an area composed of a different kind of sign? This sign is possessive in nature.

Each of these signs can be gained and lost with the amount of such gain or loss only significant in the case of altitude (although it may turn out in subsequent work that by defining a threshold say between high and low altitude (we might decide to name this 'pronouncement' or somesuch) this sign also become possessive). The images produced via physical simulation can now be analysed within this framework:

Table 5.2: Analysis of DCA output images by semiotic categories.

Image	Altitude	Altitudinal-homogeneity	Phase-regularity	Planar-completeness	Enclosure
P1: Blob-mound	High	No	No	No	Yes
P2: Blob-square	Low	No	No	Yes	No
P3: Thin-ridge small	Low	Yes	Yes	No	No
P4: Fat-ridge small	High	Yes	No	Yes	No
P5: Fat-ridge large	Low	Yes	No	No	Yes

P6: Small-pokey	Low	Yes	Yes	No	Yes
P7: Large-pokey	High	No	No	No	No

5.2.2.3 Discussion of results in the context of control data

It is important to compare the images produced by the system for the seven polymorph plaques with those produced for a simulated artery that does not contain an obstruction. These images form the control-data for the analysis and, equally importantly, allow us to see how the DCA informs us that no arterial occlusion is present.

The first point to take into account in this context is that the range of amplitudes divided up to correspond to the terms of the Maclaurin Power Series is itself computed from the input data, the idea being that the significance of fluctuation in the signal is relative to the minimum and maximum amplitude values for that particular instance of the phenomenon. For the control-recording, this range was very small but the DCA nevertheless adapted to it and produced patterns characteristic of the Greenberg-Hastings cellular automaton. Small amplitude ranges also occurred for plaques p5 and p6 and so the question arises as to how one reliably tells the

difference between these two plaque topologies and the absence of a plaque. The answer comes from the fact that, for the control-data, there is no consistent categorisation possible of given the criteria above. In general, the images have low altitude and do not exhibit altitudinal homogeneity whilst consistently exhibiting phase-regularity; this is actually not a categorisation seen in any of the seven polymorph plaques and might suffice to indicate the system's base-output on its own, however, it is also the case that the presence of planar-completeness and enclosure varies to a large extend between the base-images - something that does not occur in repeat runs for the polymorph plaques. It is important to note that this places a requirement on the user of the DCA imaging system to make repeat runs since it would otherwise be possible to confuse the absence of an occlusion with the presence of certain plaque topologies. This suggests that further work on refining the system should begin with rendering the images continuously and in real-time as the data comes in; this would allow the absence of a plaque to be identified by an unstable image consisting only of low-altitude peaks, a stable image of any other kind indicating the presence of an occlusion.

Figure 5.10: System output showing fluctuation in base-image for absence of plaque (note that peak-height has been automatically scaled-up - the peaks shown would all qualify as having ‘low’ altitude).

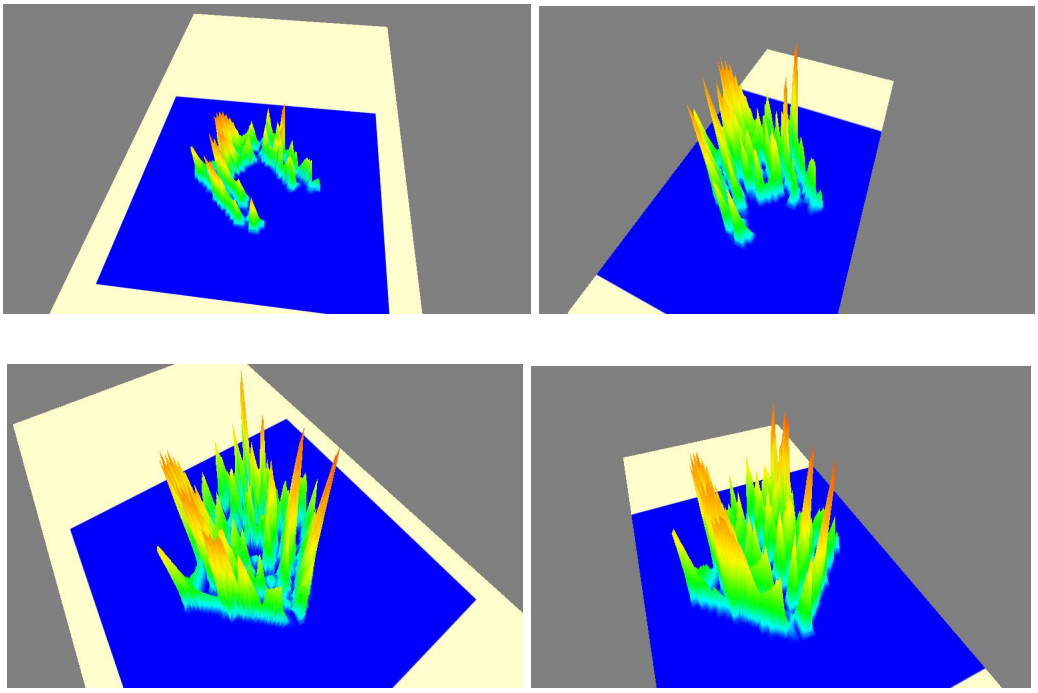

Chapter Six

Conclusions and Future Work

6.0 Conclusions and Future Work

It was discovered early in the project that, due to the physics underlying the theory of vortex-sound, there was no possibility of 'reverse-engineering' the sound recorded in order to produce images (whether 2D or 3D) of the blockage responsible for said sound (regardless of the resolution and/or overall quality of the recording). The technique of lateral-thinking therefore took a central role, first resulting in the idea to utilize the error present in the signal within the EPI framework of Frieden (2004) and then, when a straightforward way of automating the process as described by its discoverer proved unachievable, in the semio-spectral approach whereby the EPI principle was re-expressed at a higher-level of abstraction that nevertheless retained the essential elements necessary to acquire topological information that would be of use to surgeons.

In specific relation to the aims and objectives defined at the start of the project, the following conclusions can be drawn:

In terms of the state of existing medical imaging knowledge, very little is available that is of use in a situation, such as the one addressed here, whereby special-purpose hardware is not involved. The main prohibitive factor in this is the reliance of most existing medical-imaging techniques on some form of directed energy (as opposed to the ambient sound produced by turbulent blood-flow). The

secondary survey which covered techniques that are not currently in use in medical-imaging but might be of use to this project was able to provide a starting-point in the form of Frieden's EPI principle, with the subsequent utilisation of topics such as cellular automata and semiotics arising in parallel to the development of a workable, automated EPI process. The fields of numerical methods and logical systems which were originally expected to be the primary driving force behind the secondary literature-review eventually transpired to have little applicability to the EPI-approach, the review as a whole therefore proceeding firstly as an exhaustion of existing techniques followed by the identification of an approach which, while applicable, could not be applied without being re-expressed at a higher level of abstraction. This is a successful and satisfactory outcome supporting the usefulness of a two-level literature review.

Having identified the EPI-principle as the center of whatever the solution would turn out to be, a methodology was then constructed to determine how it could be applied to the imaging of atherosclerotic plaques. This methodology used a lateral approach which has subsequently been dubbed 'semio-spectral' in light of its orientation along an axis of representation from a purely numerical approach to a purely symbolic approach with the actual solution eventually being identified in between these two semiotic extremes.

Since the hybrid approach was both the final approach tried and the first

approach to be applicable to data collected from physical simulations, it is the only approach whereby this level of study was possible but it was intended, for each of the other possible approaches, that the initial application of a prototype system to said data would focus purely on whether or not reliable indications of magnitude were produced since this is a related yet less-complex problem than geometric or topological information extraction. Having demonstrated the success of the Driven Cellular Automaton within the sphere of magnitude-indication, the approach was then extended to topological information; in order to achieve a sufficient number of semiotics 'degrees of freedom' (see the table at the end of the previous chapter) it is important to note that it was necessary to take the two-dimensional images that sufficed to indicate magnitude of occlusions and extend them into the third-dimension; despite the fact that the three-dimensional images are not directly representative of the plaques it has still turned out to be necessary to allow three dimensions in order to answer the topological question.

In order to evaluate the success of the system, it was opted to take a highly pragmatic approach that was nevertheless rooted in abstract theory (the development of a parallel to Cantor's (2000) Roentgen Semiotics). This allowed both the formalisation of the initial axiomatisation of the system's output and provided the basis by which that output could be analysed by a surgeon in order to extract useful information: the identification of the five categories of secondary topological features (i.e. the features of the images produced by the system as opposed to the

features of the plaques). A corollary of this approach was that, for cases where no occlusion is present, the negative diagnosis comes not from the categorisation of the output image but from the fact that such a categorisation is not possible on repeat runs; this in turn suggested that further work on the system should begin with the provision of continuous re-rendering in real-time.

Appendix A - An example of the EPI principle at work

The following is a paraphrased version of the derivation of the physical law governing 1/f noise given in Frieden (2004) with additional explanation from the point of view of the author based on insights acquired during its study.

A signal is defined as change in amplitude with time and can be represented algebraically as X(t). Assume that $0 \le t \le T$. The Fourier spectrum of this signal is:

$$Z_T(\omega) \equiv T^{-1/2} \int_0^T dt.X(t).e^{-i\omega t} \equiv (Z(\omega),\ Z_t(\omega))$$

and the associated "periodogram" (i.e. the complex-values of the Fourier spectrum are squared giving real numbers) is:

$$I_T(\omega) = \left| Z_T(\omega) \right|^2 = Z_r^2(\omega) + Z_i^2(\omega)$$

where functions $Z_r(\omega),\ Z_i(\omega)$ are the real and imaginary parts of the $Z_T(\omega)$.

If, for the power spectrum $S(\omega) = lim_{T\to\infty} avg(I_T(\omega))$ then an approximately constant $S(\omega)$ indicates white noise. Most phenomena exhibit a varying power spectrum, of which the most common is $S(\omega) = A\omega^{-a},\ A = const.,\ a \approx 1$. This is known as 1/f

noise and phenomena that exhibit it include voltage fluctuations in resistors and biological cell membranes, traffic density on a highway, economic time series and sunspot activity.

The root problem being dealt with by the EPI approach is to determine, by examination of the error present in a measurement of some parameter θ_n the 'ideal' value for that parameter (θ_0) which is otherwise inaccessible to us. Frieden presents the following gedanken (thought) experiment to explain the concept:

Consider a musical composition, represented mathematically as $X(t)$, i.e. a signal consisting of the variation of amplitude with time. Suppose a note ω occurs in the zeroth interval (0, T_0). We want to know what this note sounds like but we weren't listening in during the zeroth interval. The problem is to work back from what we have (a note at interval n and the error involved in measuring (in this case, perhaps, hearing) these notes) to our ideal value.

We can express the ideal value as a complex number: $Z_0(\omega) \equiv \theta(\omega) \equiv (\theta_r(\omega), \theta_i(\omega))$. What we have would then be represented as $Z_n(\omega)$. Frieden asks the question "How should the mean-square error e^2 in such an estimate vary with the chosen interval n or (equivalently) time duration T_n?". What this boils down to is that we are treating the note $Z_n(\omega)$ as an inaccurate measurement of the note we want, $Z_0(\omega)$. In the context of our thought-experiment

it is reasonable to assume that we would hear, in $Z_n(\omega)$, some residual part of $Z_0(\omega)$ and that as n increases, this residual part gets smaller and smaller and thus e^2 gets larger and larger. In fact, the squared error tends toward infinity. Frieden explains that "It will turn out that the underlying PDF is Gaussian, so that optimum estimate achieves *efficiency*.". The point at which the nature of the PDF becomes apparent will become apparent later in this section and so while it sounds as though Frieden assumes a Gaussian PDF before having reason to, this is just a side-effect of the way the derivation of 1/f noise is written up. As will be seen however, the nature of the PDF is determined by comparison of the signal with a certain class of functions; this kind of comparison, which is vital to the success of the EPI derivation of the law governing 1/f spectral noise, is not something a computer can reliably perform on its own, since it requires a combination of intuition and a vast amount of prior knowledge, not to mention the fact that, for a different problem, the nature of the PDF could be found via a completely different path, i.e. there is nothing about the way in which the PDF is determined to be Gaussian that can be made generic for a computer to apply to other, unrelated problems such as the one dealt with in this project.

If the optimum estimate achieves efficiency, then this means that the data information $I = \frac{1}{e^2}$ is actually the Cramer-Rao inequality turned into an equality - i.e. it is a special case of this inequality where the Fisher information (which is what I is) is inversely proportional to the squared-error. $I \to 0$ with time which also means that

0 is its equilibrium value and this means that the EPI approach will gives us the PDF attained at equilibrium. Frieden then proceeds to express the data-information I in terms of the power spectrum $S(\omega)$, meaning that the EPI approach can be expected to give us that power spectrum obtained also at equilibrium.

Information I in terms of power spectrum $S(\omega)$

Information I is required to embody what is known about the phenomenon in question without taking into account any of the physical factors which affect a measurement of it. It it is reasonable to think of information I as the *purist* representation of the phenomenon which, in reality, will never quite match what we can measure in the physical world. For the power spectrum $S(\omega)$, Frieden derives I based upon the following known facts (or, at least, those for which he considers there is sufficient evidence to treat them as facts):

- 1/f noise exhibits long-term memory which means that the signal at two different times cannot be determined purely through the relative time difference but that they instead must depend on the absolute time values. This fits with the relationship between 1/f noise and a musical composition: It is the time elapsed since the start of the performance that determines what the

note currently being played is, at least, this is the only rule that works consistenly for every piece of music. We cannot know the same thing based upon how much time has elapsed since the note we last paid attention to. Frieden points out that such a signal is referred to as *non-stationary*.

- 1/f noise is non-stationary in its values but *is* stationary in its changes (i.e. a relative time difference is all that is needed to determine the next *change* that will occur). This property is shared between 1/f noise and the class of *intrinsic random functions* of order zero (IRF_0) and so we can treat 1/f noise as an such a process. This in turn means that it must obey a central limit theorem.

If 1/f noise obeys a central limit theorem, this means that the PDF is separable normal which in turn means that we can apply the laws governing a single random variable to every random variable involved in the phenomenon. Frieden thus proceeds to determine the Fisher information for a single, normally distributed, random variable:

$I = \int dx \frac{p'^2}{p}$ which is equivalent, via simple algebraic manipulation of the term inside the integral, to $I = \int dx\, p \left(\frac{p'}{p}\right)^2$ which is itself equivalent to taking the average of the square of the partial derivative of ln p with respect to x: $avg\left(\left(\frac{\partial ln\, p}{\partial x}\right)^2\right)$

Since we have identified the PDF for 1/f noise as separable normal, this means that the PDF is Gaussian. This allowed Frieden to derive the Fisher

information as the reciprocal of the squared standard deviation ($I = \frac{1}{\sigma^2}$) and then use another intuitive application of prior knowledge (which, again, can not be made generic in a way useful to a computer) to derive $I = \frac{2}{\sigma^2} = \frac{4}{S(\omega)}$. Since this only gives us the Fisher information for a single frequency ω , the last step is to use this particular measure of information is additive to derive the Fisher information for the signal as a whole: $I = 4\int_{\Omega} d\omega \frac{1}{S(\omega)}$. We now have the *data-information* I for 1/f noise, which is to say that we have a purist representation of what we know about the phenomenon without taking into account any factors involved in attempting to measure it. These factors are included in the *bound-information* which is derived next.

Finding information J

The fundamental mathematical goal of the EPI process is to minimise the difference between the data information I and the physical information J. We have just found an expression for the former and will actually determine the latter by finding the *physical information* (the difference between I and J) at the same time we solve the EPI equation itself. To do this, we need a generic representation of J; since we know that J must be a functional (a function of functions) of the power spectrum, we can define it thus: $J = 4\int d\omega\, F[S(\omega),\, \omega]$. This makes the physical information

K equal to the extremum of the difference between I and J:

$$K = 4\int d\omega \left[\frac{1}{S(\omega)} - F[S(\omega),\ \omega]\right] \equiv extremum$$

We solve this equation by means of the Euler-Lagrange equation, the core of what is known as the *Calculus of Variations*:

$$\frac{d}{d\omega}\left(\frac{\partial L}{\partial S'}\right) = \frac{\partial L}{\partial S}$$

L in this equation is the *Lagrangian*, the functional that represents the behaviour of a physical phenomenon. In our case, it is derived from the expression for K (above) as:

$L = \frac{1}{S} - F$ (note that this is the expression in the square brackets with the dependent variable ω removed (from the notation).

We can now use simple calculus to determine the left and right-hand sides of the Euler-Lagrange equation:

$\partial L = \frac{1}{S} - F = S^{-1} - F$ so differentiating with respect to S gives us

$-1 * S^{-2} - \frac{\partial F}{\partial S} = -\frac{1}{S^2} - \frac{\partial F}{\partial S}$ and differentiating with respect to S' gives us 0 (since there are no terms in the Lagrangian that contain S'). That also means the differentiating this last result with respect to ω (as shown in the left-hand side of the Euler-Lagrange equation) also gives us 0, since 0 is a constant. This means that the solution of the Euler-Lagrange equation is:

$$\frac{1}{S^2} + \frac{\partial F}{\partial S} = 0$$

F must therefore satisfy this equation, but it must also satisfy the EPI solution:

$$I - KJ = 4 \int d\omega \left[\frac{1}{S} - KF \right] \equiv 0$$

The micro level solution requires that the expression being integrated ($\frac{1}{S} - KF$) also holds on its own (i.e. for specific values of ω , $KF = \frac{1}{S}$). We solve this system of simultaneous equations to get the solution:

$$KF/S = -\partial F/\partial S$$

This is a well-known differential equation for which a general solution exists:

$F[S(\omega),\omega] = G(\omega)S(\omega)^{-K}$ where $G(\omega) \geq 0$ is some unknown function. The process of finding $G(\omega)$ is what derives the power-spectrum for 1/f noise:

Invariance principle

Along with the data-information I and the bound information J, the third part of the EPI process of deriving physical laws is the application of an *invariance principle* which Frieden states as "Let the combined EPI principle remain invariant in form under an arbitrary change of scale in ω.". This basically means that if we multiply the frequency by some constant factor, the EPI equation must still hold. More specifically to the case of 1/f noise, if $\omega_1 = \alpha\omega,\ \alpha > 0$ then $S_1(\omega_1).d\omega_1 = S(\omega).d\omega$ must hold. If we substitute the definition of ω_1 into this equation, we get

$S_1(\omega_1) = (1/a)S(\omega_1/a)$. We can substitute this into the EPI equation to give:

$$I_1 - KJ_1 = 4\int d\omega_1 \left[\frac{1}{S_1(\omega_1/\alpha)} - KG(\omega_1)a^K S(\omega_1/\alpha)^{-K}\right] \equiv 0$$

If we transform this via the definition of ω_1, we get

$$I_1 - KJ_1 = 4\alpha^2 \int d\omega_1 \left[\frac{1}{S(\omega)} - KG(\alpha\omega)a^{K-1}S(\omega)^{-K}\right] \equiv 0$$

If this equation must still hold in the same way as the original EPI equation for the phenomenon, that means the $G(\omega)$ must make the integrand of this latter equation proportional to that of the original EPI equation, i.e.

$$KG(\omega)S(\omega)^{-K} = KG(\alpha\omega)\alpha^{K-1}S(\omega)^{-K}$$

The K and $S(\omega)^{-K}$ cancel in this equation to yield $G(\alpha\omega) = \alpha^{1-K}G(\omega)$ for which the general solution is $G(\omega) = B\omega^{1-K}$, $B = const.$

From the general solution for F we found earlier ($F[S(\omega),\omega] = G(\omega)S(\omega)^{-K}$), substituting this definition for $G(\omega)$ gives us $F = B\omega^{1-K}S^{-K}$ and substituting this for F in the microlevel solution gives us:

$S(\omega) = A\omega^{-1}$, $A = (KB)^{1/(K-1)} = const.$ which is the power-spectrum for 1/f noise.

References

Bagnoli, F. (2008) *Boolean derivatives and computation of cellular automata.* [online]. Available from: http://arxiv.org/PS_cache/cond-mat/pdf/9912/9912353v3.pdf [Accessed 4 February 2010].

Baer, E. (1988) *Medical semiotics*. Maryland: University Press of America.

Barenblatt, G. I. (1996) *Scaling, self-similarity, and intermediate asymptotics*. New York: Cambridge University Press.

Becker (1976) *Dimensionless parameters: Theory and methodology*. Elsevier Science and Technology.

von Bertallanfy, L. (1969) *General System theory: Foundations, Development, Applications*. New York: George Braziller, Inc.

Burgess, G. (1999) Finding Approximate Analytic Solutions to Differential Equations
Using Genetic Programming. Surveillance Systems Division, Electronics and Surveillance Research Laboratory, Department of Defense,

Australia.

Burley, M. Bechkoum, K. Pearce, G. (2006) A formative survey of geometric algebra for multivariate modelling. *In UK Society for Modelling and Simulation, (2006) European Modelling Symposium, London.* London: UCL.

Brillouin, L. (2004) *Science and Information Theory*. Second edition. New York: Dover Publications.

Burley, M. Bechkoum, K. Pearce, G. (2008) An architecture for the automatic derivation of imaging equations for the visualisation of carotid arterial plaques. *In: Tenth International Conference on Computer Modeling and Simulation.* Emmanuel College, Cambridge University, Cambridge 1-3 April, pp.112-116.

Cantor, Robert M. (2000). Foundations of Roentgen semiotics. *Semiotica: Journal of the International Association for Semiotic Studies.* **131**, pp.1-18.

Chandler, Daniel (2013). *Semiotics for Beginners.* [online]. Available from: http://www.aber.ac.uk/media/Documents/S4B/semiotic.html [Acessed 16 June 2013].

Church, A. (1941) *The Calculi of Lambda Conversion*, Princeton University Press,

Princeton, NJ.

Culjat, M., Goldenberg, D., Tewari, P., Singh, R. 2010. A review of tissue substitutes for ultrasound imaging. *Ultrasound in Medicine & Biology*. pp.861-873.

Curry, H. (1958) Combinatory logic. North-holland Publishing Company.

Da Costa, N.C.A., Decio, K. & Bueno, O. (2007) Paraconsistent logics and paraconsistency. *Philosophy of logic.* pp.791-911.

Dahl, J. J., Dumont, D. M., Allen, J. D., Miller, E. M., Trahey, G. E. (2009) Acoustic radiation force impulse imaging for noninvasive characterization of carotid artery atherosclerotic plaques: a feasibility study. *Ultrasound in Medicine and Biology*. **35**(5), pp.707-716.

Damadian, R. (1971) Tumour detection by nuclear magnetic resonance. *Science*, **171**, pp.1151-1153.

de Kleer, J. & Brown, J.S., 1984. A qualitative physics based on confluences. *Artificial Intelligence.* **24**(1-3), pp.7-83.

Dellandrea, E. Makris, P. Boiron, M. Vincent, N. (2002) A medical acoustic signal

analysis method based on Zipf law. *In: International Conference on Digital Signal Processing, July 1-3, 2002, Santorini, Greece*. IEEE. pp.615-618.

Dobashi, Y. Yamamoto, T. Nishita, T. (2004) Synthesizing sound from turbulent field using sound textures for interactive fluid simulation. *Computer Graphics Forum*. **23**(3), pp.539-546.

Differ, A. (2002) Clados project. [online]. Available from: http://clados.sourceforge.net/.

Fenster, A. Blake, C. Gyacsov, I. Landry, A. Spence, J. D. (2006) 3D ultrasound analysis of carotid plaque volume and morphology. *Ultrasonics*. **44**(supplement), pp.e153-e157.

Evensen (1994) Sequential data assimilation with nonlinear quasi-geostrophic model using Monte Carlo methods to forecast error statistics. *Journal of Geophysical Research*. **99**(C5), pp.143-162.

Frieden, B. R. (2004) Science from fisher information. 2nd ed. Cambridge: Cambridge University Press.

Frieden, B. R. Gatenby, R, A. (2005) Power laws of complex systems. *Physical*

Review E. **72**, pp.036101-036111.

Gorden, N. Salmond, D. Smith, A. (1993) A novel Approach to nonlinear/non-Gaussian Bayesian State estimation. IEE Proceedings-F, **140**(2), pp. 107-113.

Gross, C. P. Steiner, C. A. Bass, E. B. Powe, N. R. (2000) Relation between prepublication release of clinical trial results and the practice of carotid endarterectomy. *Journal of the American Medical Association.* **284**(22), pp.2886-2893.

Hardy, J., Y. Pomeau and O. de Pazzis. (1973) Time evolution of a two-dimensional model system. I. Invariant states and time correlation functions. *Journal of Mathematical Physics.* **14**(12), pp.1746-1759.

Haskell, E. ed. 1972. *Full circle: The moral force of unified science,* London: Gordon and Breach.

Hedrick, W. R. Hykes, D. L. Starchman, D., E. (1995) Ultrasound Physics and Instrument. 3rd ed. Missouri: Mosby, Inc.

Hestenes, D. Sobczyk, G. (1984) *Clifford algebra to geometric calculus: A unified*

language for mathematics and physics. Dordrecht: Kluwer Academic Publishers Group.

Hodges, W. (2005) *Logic*. Second edition. Penguin global.

Howe, M. S. (2003) *Theory of vortex sound*. Cambridge: Cambridge University Press.

Ilachinski, A. (2002) *Cellular automata: a discrete universe.* London: World Scientific. p43.

Ilachinski, A. (2002b) *Cellular automata: a discrete universe.* London: World Scientific. p13.

James, J. (1993) A Calculus of Number Based on Spatial Forms. [online]. Available from: http://www.lawsofform.org/docs/jjames-thesis.txt [Accessed 17 November 2007].

Julier and Uhlmann (1997) A New Extension of the Kalman Filter to Nonlinear Phenomena.

Jumarie, G. (1990) *Relative Information Theory*. Berlin: Springer-Verlag Berlin

Heidelberg.

Kalman, R. (1960) A new approach to linear filtering and prediction problems. *Transactions of the ASME - Journal of basic engineering*, **82**(Series D), pp. 35-45.

Kingstone, L., Castonguay, M., Torres, C., Currie, G. (2013) Carotid artery disease imaging: a home-produced, easily made phantom for two- and three-dimensional ultrasound simluation. *Journal for vascular ultrasound*. **37**(2), pp.76-80.

van Leeuwen, P. (2011) Efficient nonlinear data-assimilation in geophysical fluid dynamics. *Computers and fluids*, 46, pp.52-58.

Lei, J., Bickel, P., Snyder, C. (2010) Comparison of Ensemble Kalman Filters under Non-Gaussianity. *Monthly Weather Review*, **138**(4), pp.1293-1306.

Lehmann, T. Goenner, C. Spitzer, K. (1999) Survey: interpolation methods in medical image processing. *IEEE Trans Med Imaging,* **18**(11), pp.1049-1075.

Lighthill, M. J. (1952) On sound generated aerodynamically. Part 1: General theory. *Proceedings of the Royal Society of London.* **A211**, pp.564-587.

Lopes, P. and Piedade, M. (2000) A Kalman filter approach to active noise control. *In: Proceedings: Eusipco 2000, September 4-8, Tampere, Finland.*

Mansfield, P. (1977) Multi-planar image formation using NMR Spin echoes. *Journal of Physics C: Solid State Physics*, **10**, pp.L55-L58.

Matbase (2014) Matbase. [online]. Available from: http://www.matbase.com/ [Accessed 27 July 2014].

Menard, M. Eboueya, M. (2002) Extreme physical information and objective function in fuzzy clustering. *Fuzzy Sets and Systems*, **128**(3), pp.285-303.

Natterer, F. (1999) Numerical methods in tomography. *Acta Numerica,* **8**.

nklein software (2000) *C++ template classes for geometric algebras.* <http://www.nklein.com/products/geoma/>

Nobe, A., Tokihiro, T. (2001) From cellular automaton to difference equation: a general transformation method which preserves time evolution patterns. *Journal of Physics A: Mathematical and Gen*eral, **34,** pp.L371-L379.

Oates, P. (2005) Private communication.

Pearce, G. Perkinson, N. Pritchard, L. (2005) Patent pending.

Pearce, G. Perkinson, N. (2005a) Grant Awarded for the Patent by Mercia Spinners.

Pearce, G. Perkinson, N. (2005b) Patent pending. Grant awarded by Mercia Spinners.

Post, E. (1941) The two-valued iterative systems of mathematical logic. *Annals of mathematics series #5*.

Radon, J. (1917) Über die bestimmung von funktionen durch ihre integralwerte längs gewisser mannigfaltigkeiten. *Berichte Sächsiche Akademi der Wissenschaften, Math.-Phys,* **69**, pp.262-267.

Raparia, D, Aslessi, J. Kponou, A. (1997) The algebraic reconstruction technique (ART). [online]. Physics Abstracts. [cited 1st March 2006], Accessed via <http://arxiv.org/abs/physics/9709014>

Roads, C. (2004) *Microsound*. 2nd ed. MIT Press.

Robbins, S. (2004) *Pathologic Basis of Disease*. Saunders.

Sakellarios, A. I. Stefanou, K. Siogkas, P. Tsakanikas, V. D. Bourantas, C. V.

Athanasiou, L. Exarchos, T. P. Fotiou, E. Naka, K. K. Papafaklis, M. I. Patterson, A. J. Young, V. E. Gillard, J. H. Michalis, L. K. Fotiadis, D. I. (2012) Novel methodology for 3D reconstruction of carotid arteries and plaque characterization based upon magnetic resonance imaging carotid angiography data. *Magnetic Resonance Imaging*. **30**(8), pp.1068-1082.

Sauer, T., Xu, Y. (1995) On multivariate Lagrange interpolation. *Mathematics of Computation*, **64**(211), pp. 1147—1170.

Spencer-Brown, G. (1972) *Laws of Form*. New York: Bantam Press.

Shkolinsky, Y. Averbuch, A. (2003) 3D Fourier based discrete radon transform. *Applied and Computational Harmonic Analysis.* **15**, pp.33-69.

Shoenfinkel (1924) On the building blocks of logic.

Tsangaris, S., Drikakis, D. (1989) Pulsating blood flow in an initially stressed, anisotropic elastic tube: linear approximation of pressure waves. *Medical and biological engineering and computing*. **27**(1), pp.82-88.

Srineevasan, K., Antonia, R. (1997) The phenomenology of small-scale turbulence. *Annual Review of Fluid Mechanics*. **29**, pp.435-472.

Tsoulos, I. G Solving differential equations with genetic programming. [online]. Available from: http://www.cs.uoi.gr/~lagaris/papers/PREPRINTS/DEwGE.pdf [Accessed 8 March 2004].

Van Raad, V. (2003) Frequency-space analysis of cervical images using short time Fourier transform. *In: Proceedings of the IASTED International Conference of Biomedical Engineering, June 25-27, 2003, Salzburg, Austria.*

Vanackere, G., (2000) Hl2, an inconsistency-adaptive and inconsistency-resolving logic for general statements that mights have exceptions. *Journal of Applied Non-classical Logics.* **10**(3-4).

Vedantham, R., Hunter, J. (1997) Sound wave propagation through incompressible flows. *Wave motion*, **26**(4), pp.319-328.

Vichniac, P. (1990) Boolean derivatives on cellular automata. *Physica D*, **45**(1-3), pp.63-74.

World Health Organisation (2004) Tobacco is impoverishing people and nations, WHO warns. [online]. Available from: http://www.wpro.who.int/tfi/docs/PressReleases/WNTD%20press%20releasefact%2

0sheet.pdf [Accessed 8 March 2004].

Zhang, X., Fatemi, M., Kinnick, R., Greenleaf, J. (2003) Noncontact ultrasound stimulated optical vibrometry study of coupled vibration of arterial tubes in fluids. *Journal of the Acoustic Society of America*. **113**(3), pp.1249-1257.